Thermodynamic Stability of Gas Hydrates and Cage Occupancy of Guest Molecules

Takeshi Sugahara

Division of Chemical Engineering
Graduate School of Engineering Science
Osaka University
2001

Thermodynamic Stability of Gas Hydrates and Cage Occupancy of Guest Molecules

Takeshi Sugahara

Division of Chemical Engineering
Graduate School of Engineering Science
Osaka University
2001

Preface

This dissertation work was carried out under the direction of Professor Kazunari Ohgaki at Division of Chemical Engineering, Graduate School of Engineering Science, Osaka University from 1998 to 2001.

The objective of this work is to investigate the thermodynamic properties and crystal structure of gas hydrates, which have been expected for the applications to petroleum and chemical engineering and environmental science.

The author hopes that this research would be turned to advantage in the environmental science, and that the human, to all eternity, would live on the "clean" earth peacefully.

Takeshi Sugahara

Takeshi Sugahara

Division of Chemical Engineering
Graduate School of Engineering Science
Osaka University
Toyonaka, Osaka 560-8531, Japan

Contents

General Introduction

Gas hydrates are a special case of clathrate hydrates, which are crystalline inclusion substances. Their appearance is ice-like and they are composed of the frameworks which are constructed by the hydrogen-bonded water molecules. In the cavities that arise in the framework, the 'guest' molecules are enclosed. The presence of the guest molecule in the cavities stabilizes the structure of gas hydrates. Three structures of gas hydrate are well-known, such as the structure-I, structure-II and structure-H (Ripmeester *et al.*, 1987). Some cages configure to these unit-cell structures. All the structures have one type of cage in common,

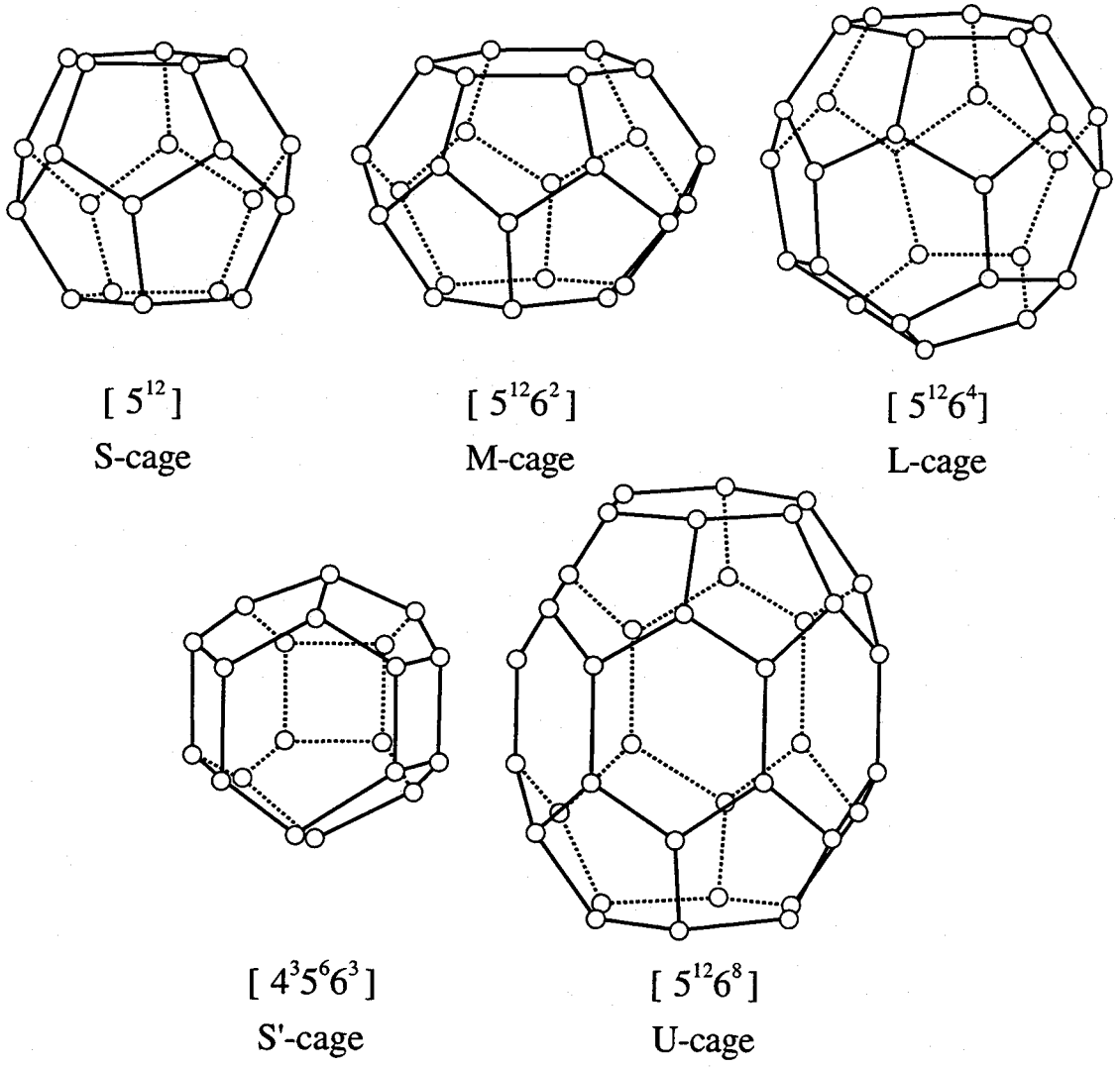

Fig. 1 Five hydrate cages constituting the structure-I, -II and -H unit cell

S-cage, which consists of pentagonal dodecahedron (5^{12}). In addition, the structure-I and structure-II have one other type of cage, which is larger than the S-cage. The structure-H has the S-cage and two other types of cages. The one is as large as the S-cage (called S'-cage), the other is much larger than S-cage (called U-cage). These cages are shown in **Fig. 1**. Circles indicate the oxygen atoms of the water molecules. The hydrogen atoms of the water molecules lie among the oxygen atoms, though they have not been drawn. The unit cell structures are summarized in **Table 1**. The structures mainly depend on the size and shape of guest speices. In this thesis, I take a great interest in the structure-I, which consists of two S-cages and six M-cages(tetrakaidecahedron, $5^{12}6^2$)(von Stackelberg, 1949) as shown in **Fig. 2** accompanied with the structure-II which consists of sixteen S-cages and eight L-cages (hexakaidecahedron, $5^{12}6^4$).

Table 1 Summary of the structure-I, -II and -H

Structures of gas hydrates							
type of unit cell	Structure-I		Structure-II		Structure-H		
water molecules in a unit cell	46		136		34		
types of cages forming unit cell	5^{12}	$5^{12}6^2$	5^{12}	$5^{12}6^4$	5^{12}	$4^35^66^3$	$5^{12}6^8$
tag of cages in this thesis	S	M	S	L	S	S'	U
number of cages	2	6	16	8	3	2	1
diameter of cages / nm	0.795	0.86	0.782	0.946	0.782	0.812	1.142
coordination number	20	24	20	28	20	20	36
diameter of free cavities / nm	0.51	0.58	0.50	0.67	0.50*	0.53*	0.86*
crystal type	Cubic		Cubic		Hexagonal		
lattice constant a / nm	1.2		1.73		1.23		
c / nm	-		-		1.02		

* subtract the diameter of water molecule from that of cage for the structure-H.

**Lattice constant for the structure-I and -II from Parrish and Prausnitz (1972), for the structure-H from Mehta and Sloan (1996)

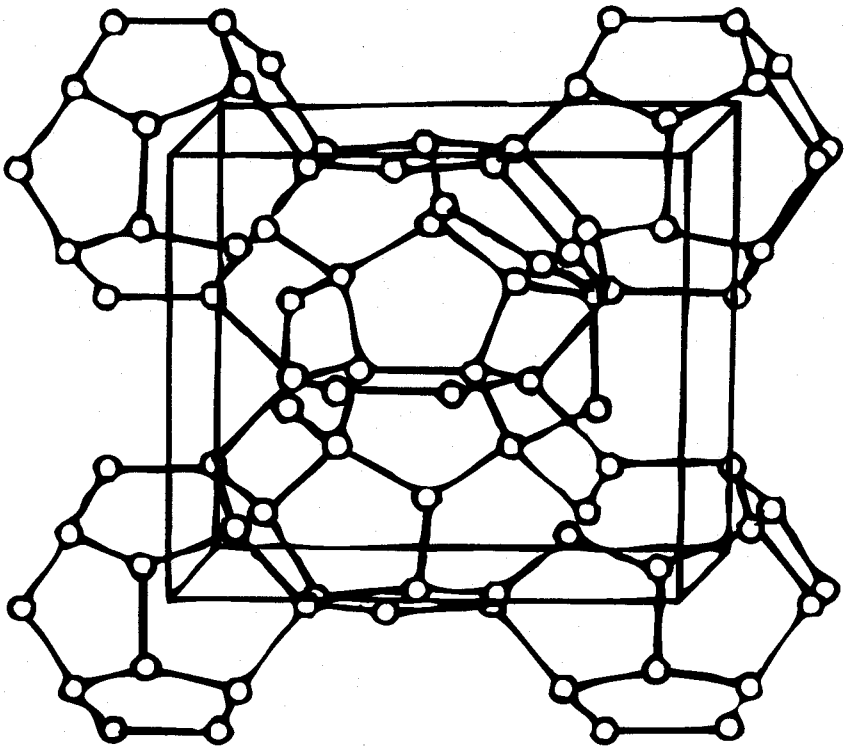

Structure-I [Pm3n]

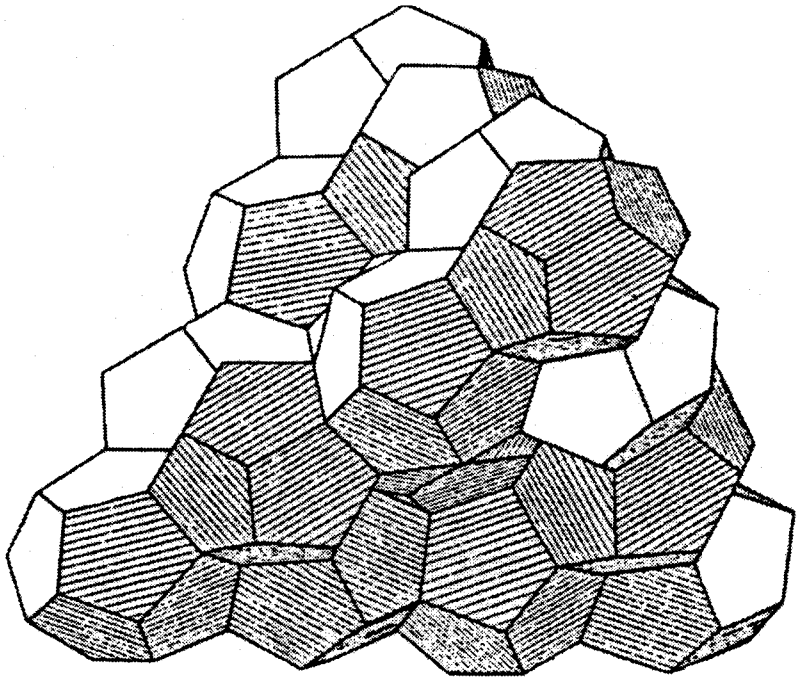

Structure-II [Fd3m]

Fig. 2 Schematic illustration of the unit cell structure-I and structure-II

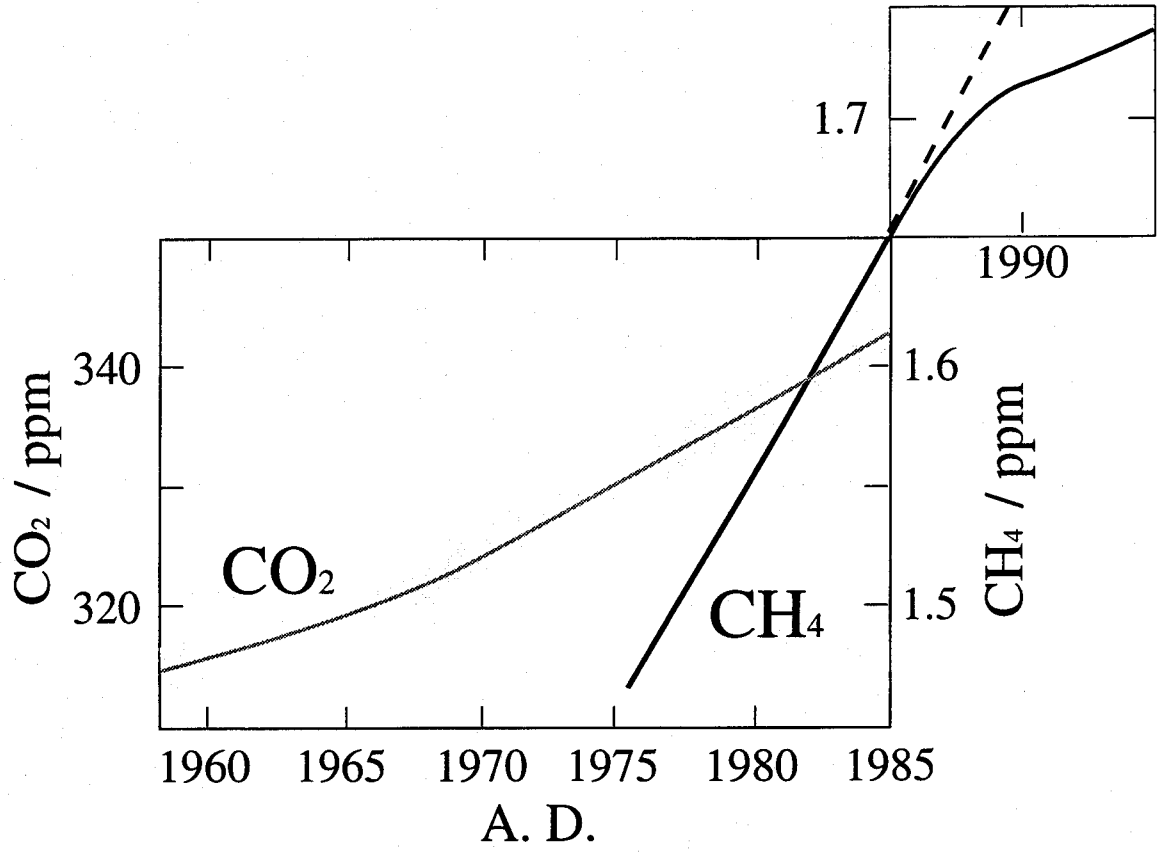

Fig. 3 Recent trend of atmospheric CO_2 and CH_4 concentration in the Northern Hemisphere (CO_2; 280 ppm : CH_4; 0.7 ppm, before the Industrial Revolution)

Since the human took the development of the steam engine in the Industrial Revolution, the human have been able to get the huge energy from the combustion of fossil fuels. During more than 200 years after the Industrial Revolution, especially in 20th century, our lifestyle was drastically changed toward the mass-production and mass-consumerization. Underneath such situation, some environmental disruptions, which were out of all knowledge such as the global warming, the acid rain, the destruction of ozone shield and the infestation of the Endocrine Disrupters, become the world-scale problems. The global warming is caused by the increase of atmospheric CO_2 concentration preventing the heat from radiating from the earth. As shown in **Fig. 3**, the atmospheric CO_2 concentration has been increasing up to 360 ppm, while it was 280 ppm before the Industrial Revolution. We must find the answer toward the solution as soon as possible.

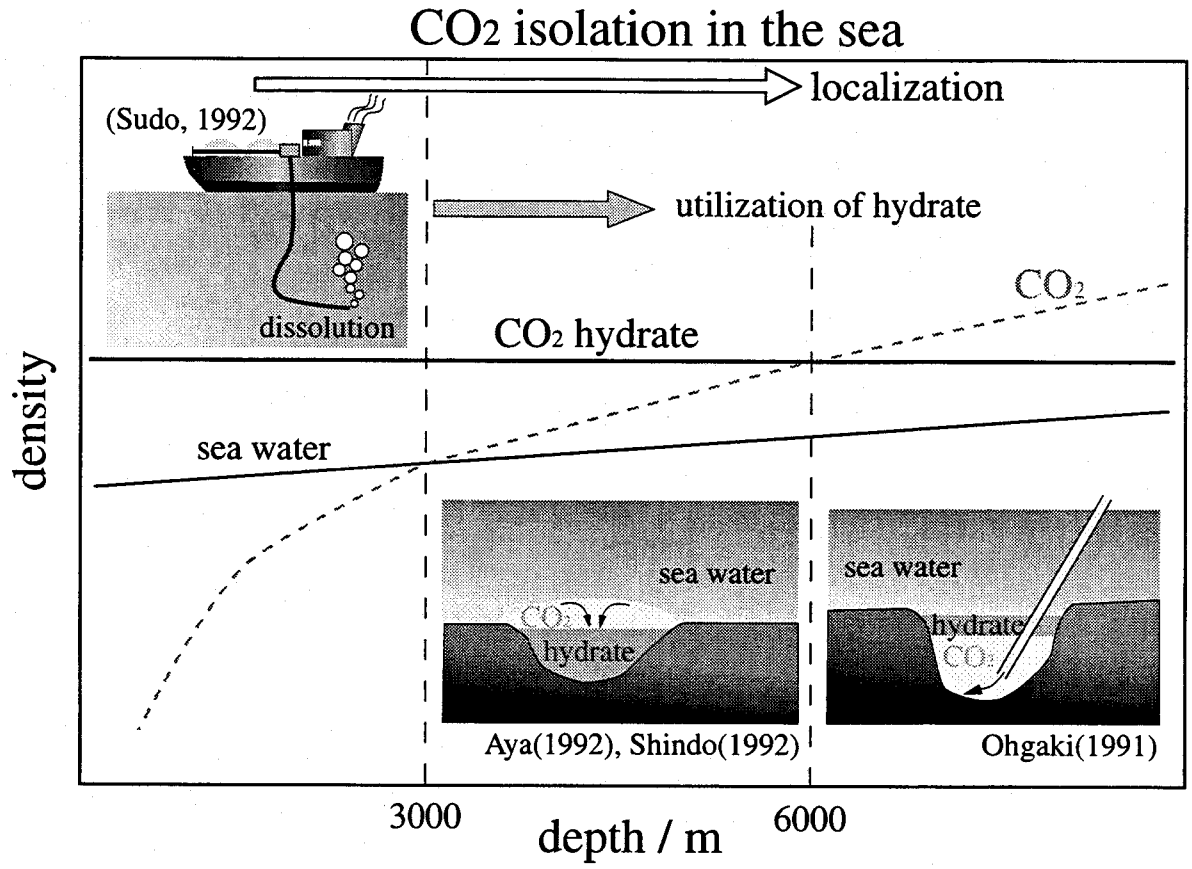

Fig. 4 Density profile of the sea water, liquid CO_2 and CO_2 hydrate. And the insets are schematic illustrations of CO_2 isolation precess in each depth,

As one of way out for the global warming, Ohgaki and Inoue(1990) proposed the CO_2 storage method on the deep ocean floor (above 6000 m in depth) using gas hydrates. In this method, the retrieved CO_2 is transported to the sensibly deep depression through the pipelines. Under the conditions of the low-temperature and high-pressure in the deep ocean, the sea water and the condensed CO_2 fluid form gas hydrates (Ohgaki *et al.*, 1993), which configurate a hydrate layer. Below the hydrate layer, CO_2 fluid condensed on the shore is pored. It is under 6000 m in depth that the density becomes larger in the order of sea water, CO_2 hydrate and liquid CO_2 (Ohgaki and Hamanaka, 1995). The profile between the density and the depth is shown in **Fig. 4**. Above 6000 m in depth, the CO_2 hydrate layer exists as the cap and plays a important role in preventing the stored liquid CO_2 from diffusing to the sea water, that is, this method is possible to store CO_2 stabler than any other method applying the ocean.

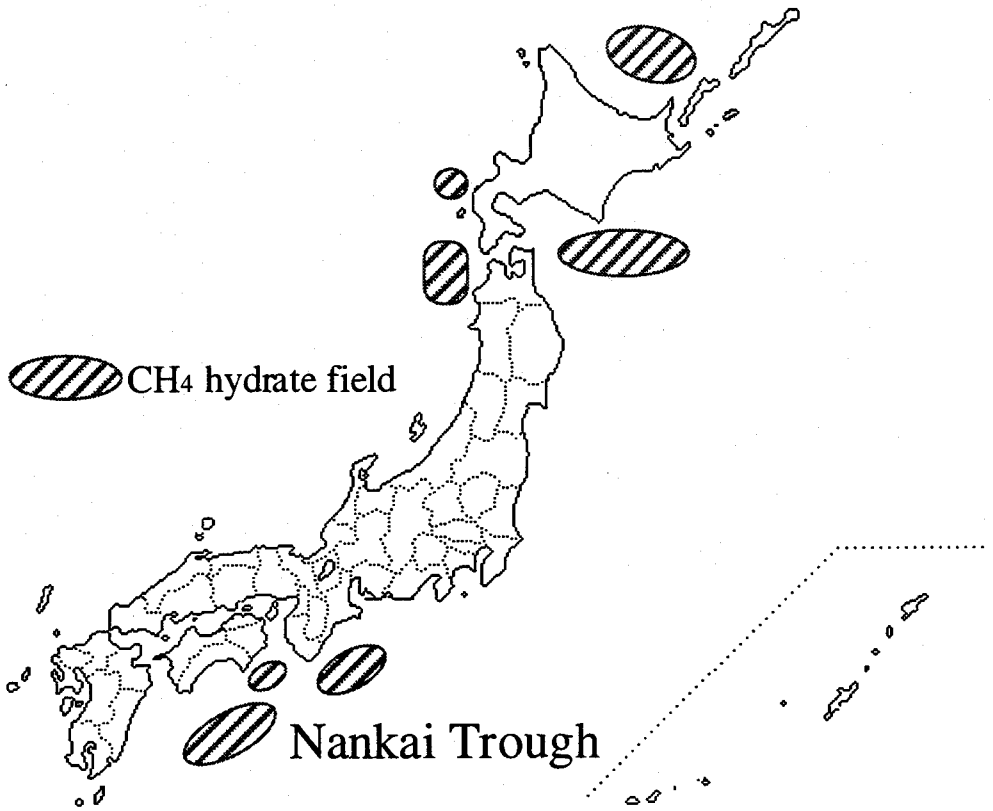

Fig. 5 Natural-gas hydrate distribution around Japan

The atmospheric concentration of CH_4 has been increased as well as that of CO_2 as shown in Fig. 3. Although its numerical amount is small, the drastic increase of atmospheric CH_4 concentration is dangerous. Because the Global Warming Potential (GWP) of CH_4 is 21 times as large as that of CO_2, CH_4 has the potential accelerating the global warming rather than CO_2. The CH_4 emission, which has been derived from natural-gas hydrates under the tundra in the Arctic and the seafloor in the world (Kvenvolden, 1988 and Englezos, 1993), is assigned as one of the origin of the atmospheric CH_4 increasing. However, such large amount of natural-gas hydrate is regarded as an unconventional and potential energy resource (Kvenvolden, 1988). The distribution of the natural-gas hydrate around Japan is shown in **Fig. 5**. In the Nankai Trough, a huge hydrate field has been espied in the depth of about 1000 m by the Bottom Simulating Reflector (BSR). The total amount of natural-gas is estimated above 200 Tmol, which corresponds to more than 100 times of the annual consumption at present in Japan. Although some exploitation methods from natural-gas hydrates have ever been proposed, however, no effective methods were anything.

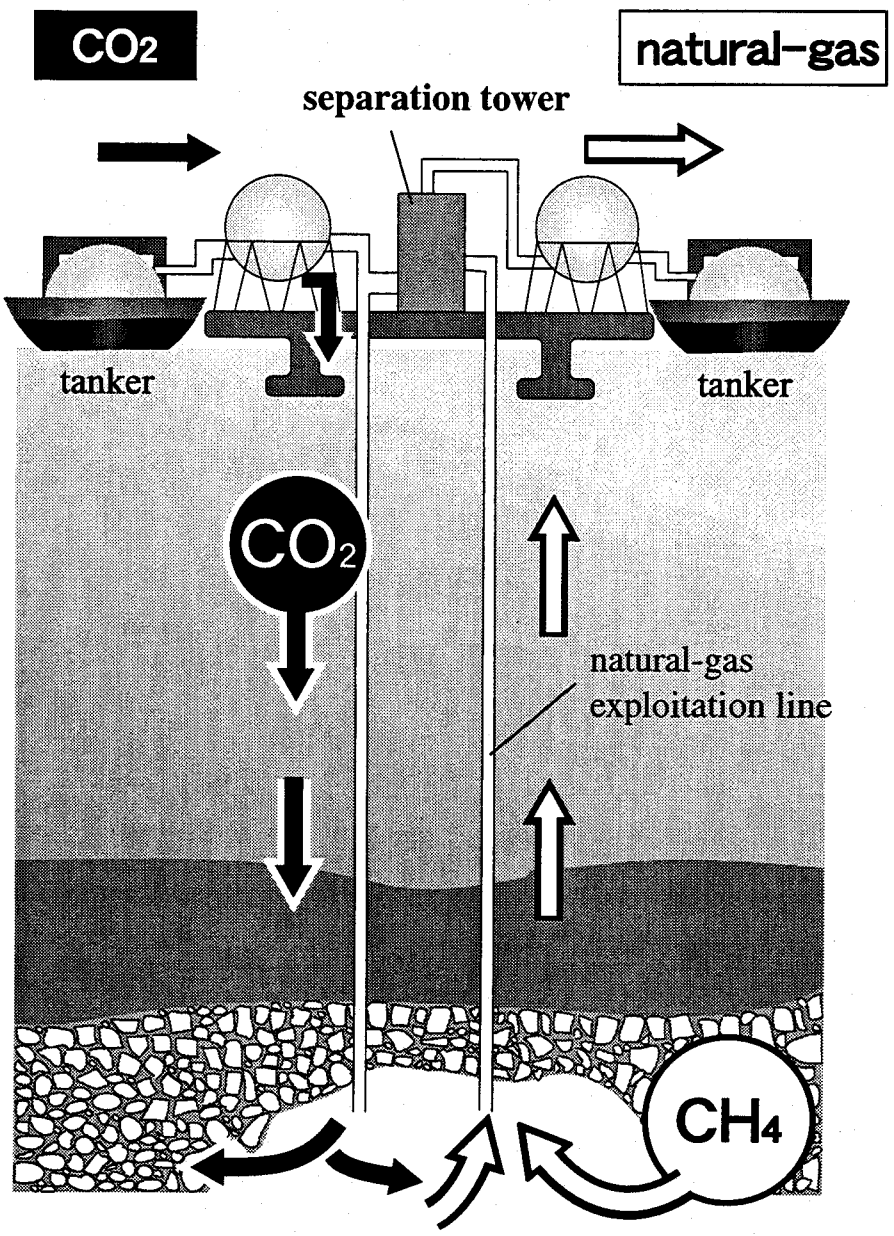

Fig. 6 Schematic illustration of the simultaneous process for the natural-gas exploitation and CO_2 isolation

Ohgaki *et al.* (1994) have proposed the methane exploitation process from such natural-gas hydrate fields in linkage with the CO_2 isolation process from our living space. Schematic illustration of this process is shown in **Fig. 6**. When the fluid CO_2 is continuously poured into the natural-gas hydrate field, the groundwater and the fluid CO_2 form the CO_2 hydrate. The heat of CO_2 hydration (which is the exothermic reaction) is larger than that of CH_4 hydrate decomposition (which is the endothermic reaction), that is, the poured CO_2 plays

an important role as the heat-supplier. Ohgaki *et al.* (1996 and 1997) suggest that this exploitation process has the potentiality from the thermodynamic view and the kinetics of CH_4 hydrate decomposition under the coexistence of CO_2. In addition, Hirohama *et al.* (1996) also suggest the feasibility of the conversion of CH_4 hydrate into CO_2 hydrate in batch system.

The discovery of crystalline gas hydrates, that were chlorine hydrates, dates back to the experiments in 1810 (Davy, 1811). For about 200 years since the presence of gas hydrate came out into the open for the first time, many investigators have made clear the structure and thermodynamical stability boundary of gas hydrates with more than 120 guest species. However high-pressure phase behavior is not examined well in respect of the stability boundary of gas hydrates. A thermodynamic understanding of gas hydrate system is essential to some practical applications, such as the natural-gas hydrate exploitation process, and the storage and transportation of natural-gas (Khokhar *et al.*, 1998).

The understanding for the structure and faculty of S-cages, which exist in all type unit cell of gas hydrates, is very significant. In the past, it has been ever believed that the CO_2, C_2H_4, C_2H_6 and cyclopropane are unable to occupy the S-cage because of their larger van der Waals diameter than that of free cavity in the S-cage. In other words, such large guest molecule can occupy only M-cage to stabilize the structure-I unit cell in the presence of vacant S-cages (Sloan, Jr., 1990). Whether CO_2 can occupy S-cages or not, especially, is one of the important knowledge in the natural-gas exploitation process using CO_2. Unfortunately, from the intramolecular C=O vibration of CO_2, the S-cage occupancy can not be discussed by means of the Raman spectroscopy because of the Fermi resonance effect. However, Morita *et al.* (2000) report that the C_2H_6 molecules, which have larger van der Waals diameter than CO_2, can occupy both the S- and M-cages from the double peaks of the C-C stretching vibration mode in hydrate phase by means of the Raman spectroscopy. This result gives many significant information that stand the common knowledge on its head, and also indicates the potentiality that CO_2 would be able to occupy the S-cages. In addition, it becomes a significant matter that the capability of S-cage occupancy,

how large molecule can occupy S-cage, is investigated.

In this thesis, thermodynamic properties and structure of gas hydrates are investigated as the fundamental studies for some practical applications using gas hydrates. In particular, the phase behavior and S-cage occupancy are the core intelligence.

In Chapter I, the high-pressure phase equilibria of the trifluoromethane (fluoroform) hydrate system were measured. Whether this hydrate system has a quadruple point of gas hydrate + water + liquid + gas phases was determined. In addition, the overall enthalpy change of hydration along the stability boundaries in this system was estimated.

In Chapter II, the high-pressure phase equilibria of the xenon hydrate system were measured. Same as Chapter I, whether this hydrate system has a quadruple point of gas hydrate + water + liquid + gas phases was determined. Compared with the phase behavior of the trifluoromethane hydrate system in Chapter I, the relationship between the quadruple point and the critical point of the pure guest molecule was discussed.

In Chapter III, the three-phase coexisting curves of ethylene hydrate system were measured. In this hydrate system, the stability boundary indicates anomalous behavior. The reason why curious behavior appears has been briefly discussed. The Raman microprobe spectroscopic analysis, moreover, was applied to investigate the microscopic structure of gas hydrates. Raman spectroscopy is a quite advantageous technique for the analysis of gas hydrate-structure. Especially, in order to discuss the occupancy of the S-cage, the intermolecular vibration between the water molecules and the intramolecular vibration energies of the guest molecules are essential. In this chapter, the single crystal of ethylene hydrate was prepared and was investigated by means of *in situ* Raman spectroscopy. The intramolecular vibration energies were measured in the ethylene hydrate phase and were compared with that of the guest fluid and aqueous phases in equilibrium. In addition, the intermolecular vibration energy between the water molecules, which configure to the hydrate cages, was measured. From these information, the S-cage occupancy and the shrinkage of hydrate cage by pressurization were discussed.

It is common knowledge that the cyclopropane is the largest molecule in some hydrate systems which configure to the structure-I. In Chapter IV, the three-phase coexisting curves of cyclopropane hydrate system were measured. By means of the Raman spectroscopy, the S-cage occupancy, its pressure-dependence and the shrinkage of hydrate cage by pressurization were discussed.

Through many investigations for the formation-mechanism and structure of gas hydrates, the existence of hydrate precursors has ever been suggested. Pauling (1959) first introduced the geometry of the basic water structure "buckyballs". The "buckyball" includes twenty one water molecules, twenty of which form a pentagonal dodecahedra (like S-cage) and one water molecule in the middle to add stability to the cage. Englezos and Bishnoi(1988) conclude that the increase in solubility of the gas in water is due to the cluster formation in the liquid state prior to the appearance of the stable hydrate phase. Lekvam and Ruoff (1993) propose the reaction kinetic model for methane hydrate, where is assumed to be the existence of the hydrate precursor. Song *et al.* (1997) indicate the existence of the structure in water based on the solubility measurements of methane and ethane in water at and near hydrate conditions. In Chapter V, the pressure-hysteresis of the methane hydrate system was investigated by means of the Raman spectroscopy and visual observation. From these results, the structure in liquid water was briefly discussed.

The results obtained in this work are summarized in General Conclusions.

Literature Cited

Englezos, P. and P. R. Bishnoi, "Free Energy Analysis for the Supersaturation Limits of Methane in Liquid Water and Hydrate-Gas-Liquid Phase Behavior," *Fluid Phase Equilibria*, **42**, 129-140 (1988)

Englezos, P., "Clathrate Hydrates," *Ind. Eng. Chem. Res.*, **32**, 1251-1274 (1993)

Davy, H., *Phil. Trans. Roy. Soc. London,* **101**, 1- (1811)

Hirohama, S., Y. Shimoyama, A. Wakabayashi, S. Tatsuta and N. Nishida, "Conversion of CH_4-Hydrate to CO_2-Hydrate in Liquid CO_2," *J. Chem. Eng. Japan*, **29**(6), 1014-1020 (1996)

Khoklar, A. A., J. S. Gudmundsson and E. D. Sloan, "Gas Storage in Structure H Hydrates," Fluid Phase Equilibria, **150-151**, 383-392 (1998)

Kvenvolden, K. A., "Methane Hydrate - A Major Reservoir of Carbon in the Shallow Geosphere?," *Chem. Geology*, **71**, 41-51 (1988)

Lekvam, K. and P. Ruoff, "A Reaction Kinetic Mechanism for Methane Hydrate Formation in Liquid Water," *J. Am. Chem. Soc.*, **115**, 8565-8569 (1993)

Mehta, A. P. and E. D. Sloan, " Improved Thermodynamic Parameters for Prediction of Structure H Hydrate Equilibria," *A.I.Ch.E. Journal*, **42**(7), 2036-2046 (1996)

Morita, K., S. Nakano and K. Ohgaki, "Structure and Stability of Ethane Hydrate Crystal," *Fluid Phase Equilibria*, **169**, 167-175 (2000)

Ohgaki, K. and Y. Inoue, "A Proposal for Gas Storage on the Ocean Floor Using Gas Hydrates," *Kagaku Kogaku Ronbunshu*, **17**(5), 1053-1055 (1990)

Ohgaki, K., Y. Makihara and K. Takano, "Formation of CO_2 Hydrate in Pure and Sea Waters," *J. Chem. Eng. Japan*, **26**(5), 558-564 (1993)

Ohgaki, K., K. Takano and M. Moritoki, "Exploitation of CH_4 Hydrates under the Nankai Trough in Combination with CO_2 Storage," *Kagaku Kogaku Ronbunshu*, **20**(1), 121-123 (1994)

Ohgaki, K. and T. Hamanaka, "Phase-Behavior of CO_2 Hydrate - Liquid CO_2 - H_2O System at High Pressure," *Kagaku Kogaku Ronbunshu*, **21**(4), 800-803 (1995)

Ohgaki, K., K. Takano, H. Sangawa, T. Matsubara and S. Nakano, "Methane Exploitation by Carbon Dioxide from Gas Hydrates - Phase Equilibria for CO_2-CH_4 Mixed Hydrate System -," *J. Chem. Eng. Japan*, **29**(3), 478-483 (1996)

Ohgaki, K., S. Nakano, T. Matsubara and S. Yamanaka, "Decomposition of CO_2, CH_4 and CO_2-CH_4 Mixed Hydrates," *J. Chem. Eng. Japan*, **30**(2), 310-314 (1997)

Parrish, W. R. and J. M. Prausnitz, "Dissociation Pressures of Gas Hydrates Formed by Gas Mixtures," *Ind. Eng. Chem. Process Des. Develop.*, **11**(1), 26-35 (1972)

Pauling, L., "The Structure of Water. Hydrogen Bonding," Hadzi, D. (ED.), Pergamon Press (1968)

Ripmeester, J. A., J. S. Tse, C. I. Ratcliffe and B. M. Powell, "A New Clathrate Hydrate Structure," *Nature*, **325**, 135-136 (1987)

Sloan, E.D. Jr.; Clathrate Hydrates of Natural Gases, Dekker, New York, U.S.A. (1990)

Song, K. Y., G. Feneyrou, F. Fleyfel, R. Martin, J. Lievois and R. Kobayashi, "Solubility Measurements of Methane and Ethane in Water at and near Hydrate Conditions," *Fluid Phase Equilibria*, **128**, 249-260 (1997)

von Stackelberg, M. V., "Feste Gashydrate," *Naturwissenschaften*, **36**, 327-333 (1949)

Chapter I

Border Gas Hydrate System Having Quadruple Point of Hydrate + Two Liquids + Gas Phases

Abstract

Four three-phase coexisting curves for the trifluoromethane hydrate system were obtained over a pressure range up to 72 MPa and temperature range from 283 to 302 K. Two invariant points determined in the present study are the critical end point of 299.44 K and 4.85 MPa, and the quadruple point of 292.25 K and 4.07 MPa. The former, where the gas and liquid are critically identical in the presence of water phase, is located very close to the critical point of the trifluoromethane fluid. The latter is the origin of four three-phase coexisting curves. The overall enthalpy change of hydration is estimated over the whole temperature region. The important finding is that trifluoromethane hydrate is the border system having a quadruple point (hydrate+two liquids+gas) in a series of critical temperatures of known guest species. It is also identified that xenon hydrate is the opposite border system having no quadruple point. (This was explained in full detail in Chapter 2.)

Introduction

The structure and thermodynamic properties of gas hydrates have been studied by many investigators for about 200 years. Recently, gas hydrates have attracted much attention from petroleum and chemical engineering and earth and environmental scientists. It is well-known that more than 120 guest species are able to stabilize the ice-like clathrate hydrates. However high-pressure phase behavior is not examined well in respect of the stability boundary of gas hydrates. A thermodynamic understanding of gas hydrate system is essential to such practical applications.

In the language of pressure-temperature projection, the phase diagrams of gas hydrate systems can be divided broadly into two groups, depending on the invariant quadruple points of $Q_1(H+S_1+L_1+G(F))$ and $Q_2(H+L_1+L_2+G)$. The symbols H, S, G and F stand for the gas hydrate phase, the solid phase, the gas phase and the fluid phase, respectively. Also the symbol L_1 is chosen to represent a liquid phase where the mole fraction of water is larger than that of the guest molecule fluid, L_2, in equilibrium.

I have investigated three-phase coexisting curves to elucidate the phase behavior of the gas hydrate systems. The quadruple point Q_2 plays the important role of distinguishing the phase diagram of the gas hydrate systems. The critical temperature of the guest molecule is a primary index for determining the type of phase diagrams. The sequence relating to the critical temperatures of the guest molecules is as follows; ethylene (282.4 K), xenon (289.7 K), trifluoromethane (299.3 K), and carbon dioxide (304.1 K). It is expected that the gas hydrate systems of such guest molecules lie in the transitional zone whether the quadruple point Q_2 appears (type-q_2 diagram) or not (type-q_1 diagram). In this chapter, the thermodynamical stability boundaries for the trifluoromethane(fluoroform, CHF_3) hydrate system were measured to make clear what is the border hydrate system having the quadruple point Q_2.

As experimental strategy, I pay much attention to the critical end point located near the critical point of the pure guest fluid. When the critical end point is described as $(H+L_2=G)$, where the gas and liquid phases are critically identical in the presence of the hydrate phase, the hydrate system is identified to belong to the type-q_1 diagram. On the other hand, the type-q_2 diagram has the critical end point of $(L_1+L_2=G)$.

In the present study, each three-phase coexisting curve of the trifluoromethane hydrate system is measured to make clear what type diagram the trifluoromethane gas hydrate system belongs to. In addition, four three-phase coexisting curves of $(H+L_1+G)$, $(H+L_1+L_2)$, $(H+L_2+G)$ and (L_1+L_2+G) are measured in a pressure range up to about 72 MPa and temperature range from 283 to 302 K.

1.1. Experimental

1.1.1. Material

Research grade trifluoromethane of purity above 99.999 mol% was obtained from Takachiho Trading Co., Ltd. and used without further purification. The distilled water was obtained from Yashima Pure Chemical Co. Ltd..

1.1.2. Experimental Apparatus

The experimental apparatus used in this study is essentially the same as the previous one (Ohgaki and Hamanaka, 1995). Schematic diagram of the experimental apparatus used in this chapter was shown in **Fig. 1-1**. It consists of several parts; a high-pressure cell having sapphire windows, a mixing ball operated by a vibrator, a high-pressure pump for supplying and/or pressurizing the samples, an intensifier, a pressure gage, temperature control systems, and a charge-coupled device (CCD) camera. The high-pressure optical cell was made of heat-treated stainless steel (SUS 630). The cell had inner volume of approximately 1 cm^3 and

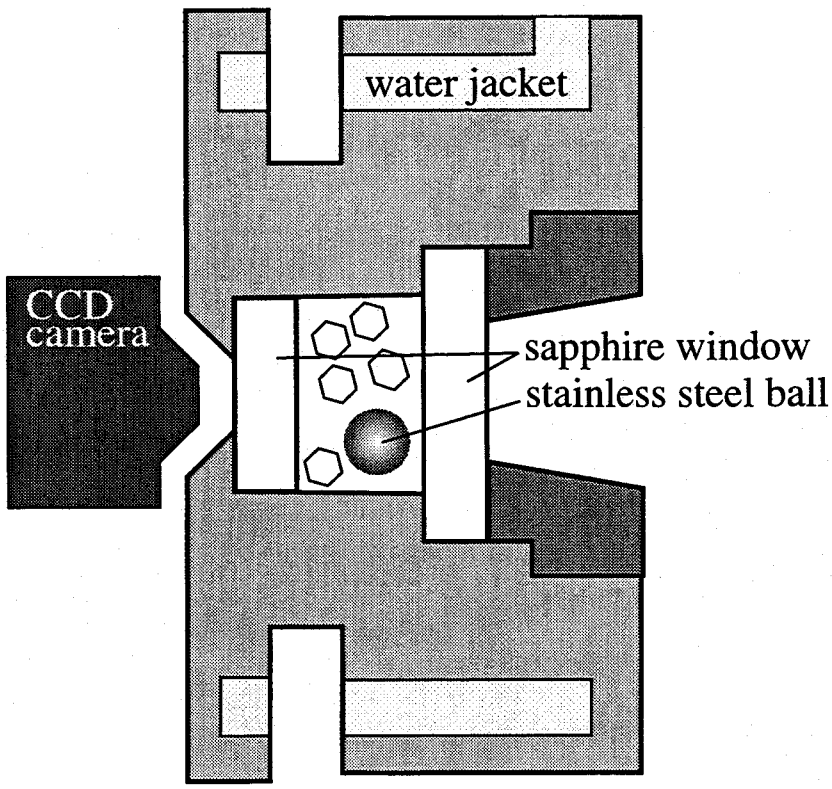

Fig. 1-1 Schematic diagram of high-pressure cell in the sectional direction.

the maximum working pressure was about 75 MPa. A pair sapphire windows, whose thickness and diameter was 4 mm and 16 mm, respectively, was set on both sides of the inner volume. Each window was sealed with a packing made of Teflon type material. A stainless steel ball of 5 mm in diameter was enclosed with the inner space to agitate the system by vibration from outside.

The system temperature was controlled by the thermostated water circulating from a thermocontroller(TAITEC CL80 + TAITEC PU-9) thorough the jacket in the cell.

The water was pressurized by means of a high-pressure pump (Shimadzu LC-10AT) up to 25 MPa, and further pressurization was performed by means of the intensifier whose sectional area ratio was about 3:1. The phase behavior was observed by a CCD camera through the sapphire window.

1.1.3 Experimental procedures

The trifluoromethane was introduced into a vacuumed cell. Then, the contents were pressurized up to a desired pressure by successively supplying water or by controlling the inner volume. After the formation of the trifluoromethane hydrate, the system temperature was gradually increased to establish the three-phase coexisting state. Phase behavior was observed by a CCD camera through a sapphire window. The equilibrium temperature was measured within an accuracy of $\pm$ 0.01 K using a thermistor probe calibrated by a Pt resistance thermometer (Takara D-641). The equilibrium pressure was measured using a pressure gage (Valcom VPRT) calibrated by a RUSKA quartz Bourdon tube gage within an accuracy of $\pm$0.01 MPa.

1.2. Results and Discussion

The experimental pressure-temperature relations of the phase boundaries for the trifluoromethane hydrate system investigated in this study are listed in **Table 1-1** and shown in **Fig. 1-2**. The ($H+L_2+G$), (L_1+L_2+G) and ($H+L_1+G$) curves agree with the literature value (Kubota *et al.* 1984). The ($H+L_2+G$) and (L_1+L_2+G) curves lie slightly below the saturated vapor-pressure curve of the

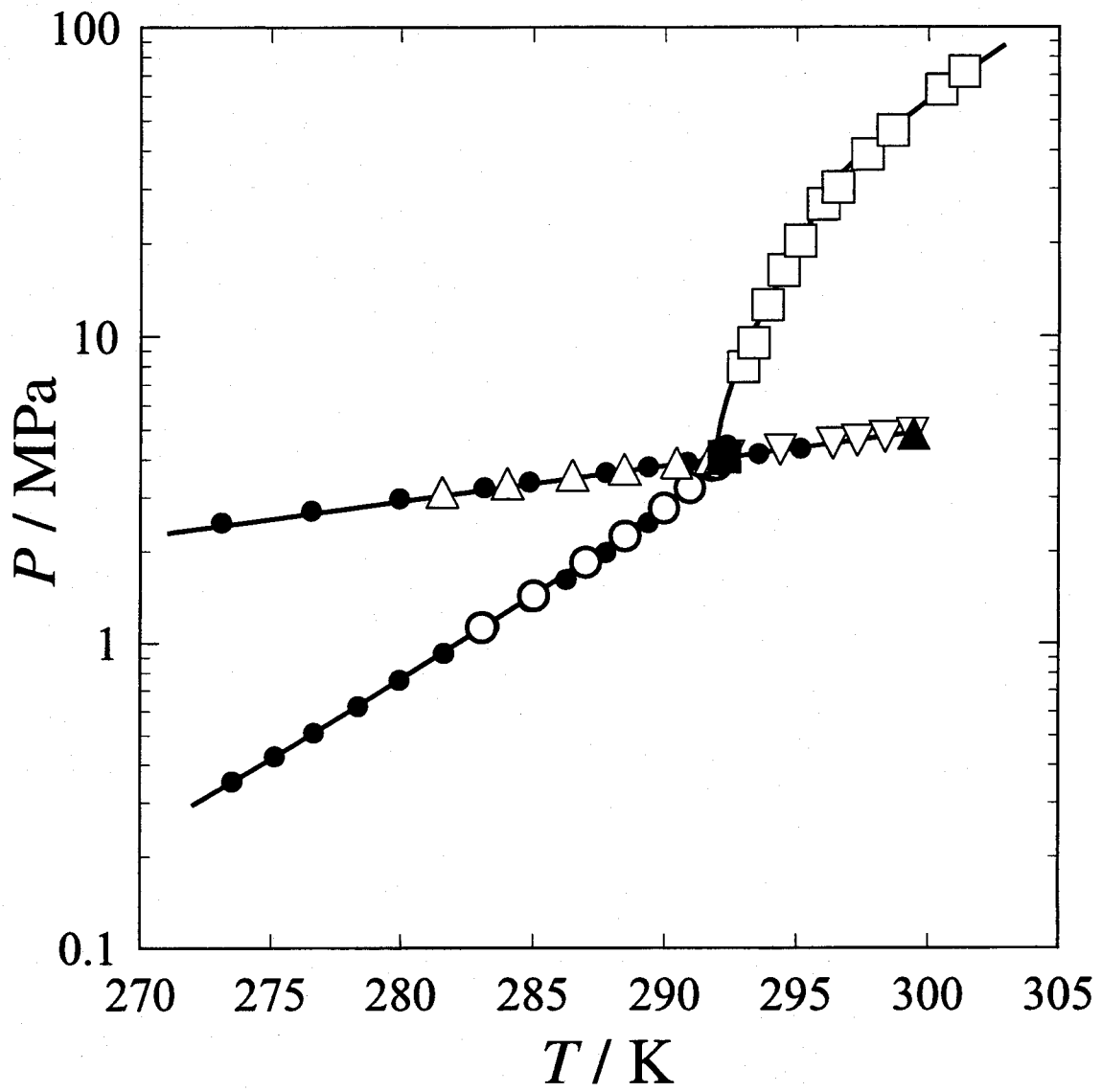

Fig. 1-2 Three-phase coexisting curves of trifluoromethane hydrate system: O, $H+L_1+G$; Δ, $H+L_2+G$; □, $H+L_1+L_2$; ▽, L_1+L_2+G; ■, quadruple point (Q_2); ▼, critical end point ($L_1+L_2=G$); ●, Kubota *et al.* (1984)

trifluoromethane fluid. The ($H+L_2+G$) curve intersects the ($H+L_1+G$) curve at the quadruple point $Q_2(H+L_1+L_2+G)$ of 292.25 K and 4.07 MPa. The (L_1+L_2+G) curve having no hydrate phase terminates at the critical end point($L_1+L_2=G$) of 299.44 K and 4.85 MPa, that is close to the trifluoromethane critical point of 299.3 K and 4.86 MPa. Namely, the temperature of the critical end point($L_1+L_2=G$) is about 7 K higher than that of the quadruple point $Q_2(H+L_1+L_2+G)$. As the trifluoromethane hydrate system has the critical end point of ($L_1+L_2=G$), this

system is identified to belong to the type-q_2 diagram as shown in **Fig. 1-3**.

As forementioned, the sequence relating to the critical temperatures of the guest fluids is ethylene (282.4 K) < xenon (289.7 K) < trifluoromethane (299.3 K) < carbon dioxide (304.1 K). The trifluoromethane and carbon dioxide hydrate systems belong to the type-q_2, while the ethylene and xenon hydrate systems belong to the type-q_1 (shown in Chapter 2). That is, the border hydrate system having the quadruple point Q_2 is the trifluoromethane hydrate system.

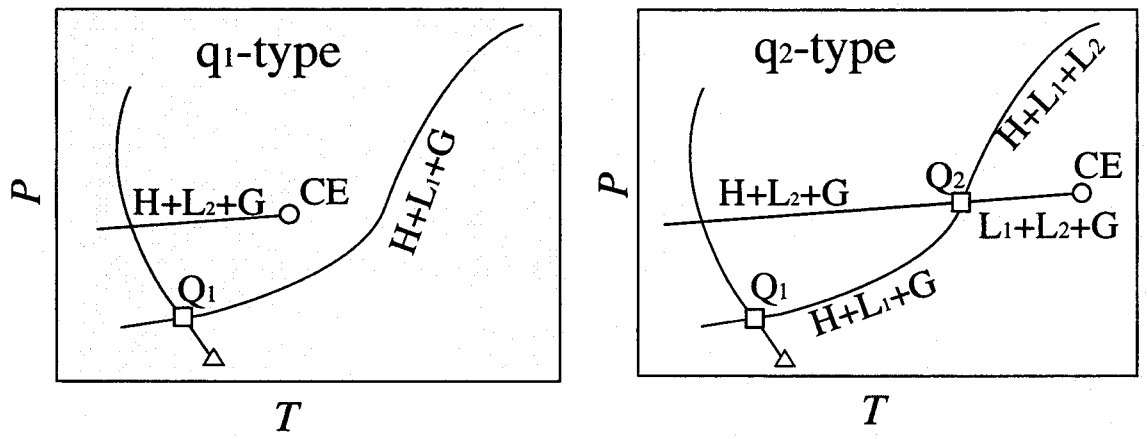

guest species	critical temperature	critical end point	quadruple point H+L1+L2+G
C_2H_4	282.4 K	H+L2=G 282.73 K, 5.03 MPa	———
Xe	289.7 K	H+L2=G 289.76 K, 5.86 MPa	———
CHF_3	299.3 K	L1+L2=G 299.44 K, 4.85 MPa	292.25 K, 4.07 MPa
CO_2	304.1 K	L1+L2=G ~304.1 K, 7.38 MPa	283.22 K, 4.5 MPa

Fig. 1-3 Classification of phase diagram for gas hydrate systems

Table 1-1 Three-phase coexisting curves of trifluoromethane hydrate system

T / K	p / MPa	T / K	p / MPa
H+L_1+G		H+L_2+G	
283.07	1.13	281.58	3.13
285.02	1.43	284.02	3.33
286.99	1.84	286.48	3.55
288.47	2.25	288.45	3.71
289.95	2.77	290.43	3.89
290.94	3.23	291.72	4.02
291.94	3.93	292.11	4.06
292.13	3.98		
H+L_1+L_2		L_1+L_2+G	
292.97	7.97	292.40	4.09
293.36	9.53	294.38	4.29
293.89	12.67	296.37	4.49
294.49	16.39	297.30	4.59
295.12	20.37	298.35	4.72
296.00	26.74	299.39	4.84
296.55	30.33	Critical end point	
297.67	38.75	299.44	4.85
298.63	46.34		
300.50	62.76	Quadruple point	
301.38	71.78	292.25	4.07

The slope of $(dp/dT)_{equil.}$ was calculated at each data point on the $(H+L_1+G)$ and $(H+L_1+L_2)$ curves. From the combination of $(dp/dT)_{equil.}$ and molar volume of the trifluoromethane hydrate, water and compressed trifluoromethane fluid, we can obtain the overall enthalpy change ΔH_{hyd} by using the Clausius-Clapeyron equation:

$$\left(\frac{dp}{dT}\right)_{equil.} = \frac{\Delta H_{hyd}}{\Delta v_{hyd} T} \qquad (1\text{-}1)$$

The total volume change Δv_{hyd} is defined by Eq. (2):

$$\Delta v_{hyd} = v^{F}_{CHF_3} + \lambda \cdot v^{L}_{H_2O} - v^{H} \qquad (1\text{-}2)$$

where v^{H} was calculated from the lattice constant of 1.20 nm (von Stackelberg, 1949) and $v^{F}_{CHF_3}$ was obtained from the Lee-Kesler equation of state (Reid, *et al.*, 1987). The hydration number λ was assumed to be 5.75 (ideal hydrate), which denotes that the trifluoromethane molecule can occupy both S- and M-cages. The overall enthalpy change ΔH_{hyd} over the entire temperature range of both $(H+L_1+G)$ and $(H+L_1+L_2)$ regardless of the quadruple point Q_2 is listed in **Table 1-2**. The ΔH_{hyd} becomes a continuous line in the $(H+L_1+G)$ and $(H+L_1+L_2)$ regions.

Table1-2 Overall enthalpy change of trifluoromethane hydrate formation

T / K	Δv_{hyd} / $cm^3 \cdot mol^{-1}$	dp/dT / $MPa \cdot K^{-1}$	ΔH_{hyd} / $kJ \cdot mol^{-1}$
	H+L_1+G		
285.02	1404	0.1708	68.3
286.99	1040	0.2263	67.5
288.47	808.9	0.3106	72.5
289.95	603.7	0.4314	75.5
290.94	469.4	0.5326	72.7
	H+L_1+L_2		
292.97	49.48	5.336	77.3
293.36	47.73	5.545	77.6
293.89	45.14	5.829	77.3
294.49	43.00	6.150	77.9
295.12	41.29	6.487	79.1
296.00	39.23	6.958	80.8
296.55	38.32	7.253	82.4
297.67	36.56	7.852	85.5
298.63	35.30	8.366	88.2
300.50	33.20	9.367	93.4
301.38	32.27	9.838	95.7

* the data around the quadruple point are neglected

Summary

Four three-phase coexisting curve of ($H+L_1+G$), ($H+L_1+L_2$), ($H+L_2+G$) and (L_1+L_2+G) for the system of the trifluoromethane hydrate have been determined in the temperature range from 283 to 302 K and pressure range up to 72 MPa. The invariant quadruple point of $Q_2(H+L_1+L_2+G)$ is located at 292.25 K and 4.07 MPa. The (L_1+L_2+G) curve terminates at the invariant critical end point ($L_1+L_2=G$) of 299.44 K and 4.85 MPa. The existence of the critical end point of ($L_1+L_2=G$) reveals that the trifluoromethane hydrate system belongs to category q_2, which has a quadruple point of $Q_2(H+L_1+L_2+G)$ as well as $Q_1(H+S_1+L_1+G)$. The ΔH_{hyd} shows weak temperature-dependency and becomes a continuous line in the ($H+L_1+G$) and ($H+L_1+L_2$) regions.

One of the most important findings in the present study is that trifluoromethane has the lowest critical temperature among the known guest molecules which form gas hydrates of type-q_2 diagram. That is, the trifluoromethane hydrate is the border system having the quadruple point Q_2 in a series of critical temperatures of the guest species.

Nomenclature

H	=	enthalpy of the hydration	[J/mol]
p	=	pressure	[Pa]
T	=	temperature	[K]
v	=	molar volume	[m^3/mol]

< Greek >

λ	=	hydration number	[-]

<Symbols>

F	=	fluid phase
G	=	gas phase
H	=	hydrate phase
L	=	liquid phase
S	=	solid phase

<Subscripts>

1	=	host component(water)
2	=	guest component(trifluoromethane)
hyd	=	hydration

Literature Cited

Kubota, H., K. Shimizu, Y. Tanaka and T. Makita, "Thermodynamic Properties of R13 ($CClF_3$), R23 (CHF_3), R152a ($C_2H_4F_2$) and Propane Hydrates for Desalination of Sea Water," *J. Chem. Eng. Japan*, **17**(4), 423-429(1984)

Ohgaki, K., and T. Hamanaka, "Phase-Behavior of CO_2 Hydrate-Liquid CO_2-H_2O System at High Pressure," *Kagaku Kogaku Ronbunshu*, **21**, 800-803(1995)

Reid, R. C., J. M. Prausnitz and B. E. Poling, The Properties of Gases & Liquids, 4th ed., p.47-49, McGraw-Hill Book Company, New York, USA (1986)

von Stackelberg, M., "Feste Gashydrate," *Naturwissenschaften*, **36**, 327-333 (1949)

Chapter II

Thermodynamical Stability Boundary for the Xenon Hydrate System

Abstract

The thermodynamical stability boundaries for the Xe hydrate system were investigated in a pressure range up to 70 MPa and a temperature range from 290 to 320 K. In the critical temperature series of the guest molecules, the Xe hydrate is identified to be the border hydrate system having no quadruple point of (hydrate + two liquids + gas). The three-phase coexisting curve of (hydrate + liquid Xe + gas) terminates at the critical end point (289.76 K, 5.86 MPa) of (hydrate + liquid = gas) very close to the critical point of pure Xe fluid. The three-phase coexisting curve of (hydrate + water + gas) exhibits the characteristic "S-shape" as if there would exist the quadruple point. The enthalpy change of Xe hydration was also evaluated from the Clausius-Clapeyron equation, the average value of 65 kJ/mol is almost constant in the whole temperature range along with the three-phase coexisting curve.

Introduction

Gas hydrates have recently attracted much attention of many investigators of petroleum and chemical engineering and environmental science. A thermodynamic understanding of gas hydrate system is essential to such practical applications.

In the language of pressure-temperature projection, the phase diagrams of gas hydrate systems can be divided broadly into two groups, depending on the invariant quadruple points of $Q_1(H+S_1+L_1+G)$ and $Q_2(H+L_1+L_2+G)$. The symbols H, S and G stand for the gas hydrate phase, the solid phase and the gas phase, respectively. Also the symbol L_1 is chosen to represent a liquid phase where the

mole fraction of water is larger than that of the guest molecule fluid, L_2, in equilibrium.

In the type-q_1 diagram corresponding to only one quadruple point Q_1, the three-phase coexisting curve ($H+L_2+G$) terminates at the critical end point ($H+L_2=G$), where the gas and liquid phases are critically identical in the presence of a hydrate phase, before it intersects the three-phase coexisting curve ($H+L_1+G$). The type-q_2 diagram has two quadruple points of Q_1 and Q_2. The critical temperature of the guest molecule is a primary index for determining the type of phase diagrams. If we write down the guest molecules in order of their critical temperatures, C_2H_4(282.4 K), Xe(289.7 K), CHF_3(299.3 K) and CO_2(304.1 K) would lie in the transitional zone between the type-q_1 and the type-q_2. The C_2H_4 hydrate system has been identified to belong to the type-q_1 while the CO_2 and CHF_3 hydrate systems belong to the type-q_2. It is still unclear which category the Xe hydrate system belongs to.

Moreover, Xe as well as H_2S are well known guest molecules called "help-gas" which can enter the smaller hydrate cage (S-cage) and stabilize the mixed hydrate crystal. For the investigation on the hydration mechanism, the gas hydrates of such guest molecule are very important. However, the phase behavior or stability boundary for the pure Xe hydrate system is not examined well, especially, in the high pressure region.

In the present study, two stability boundaries of ($H+L_2+G$) including the critical end point and ($H+L_1+G$) have been determined by straightforward visual observation in a temperature range from 290 to 320 K and a pressure range up to 70 MPa.

2.1 Experimental

2.1.1 Material

Xenon was purchased from Daido Hoxan Inc., having a stated minimum purity of 99.995 mol%. Majority of the impurity was Krypton that measured 3.78 ppm. The distilled water was obtained from Yashima Pure Chemical Co. Ltd..

2.1.2 Experimental Apparatus

The experimental apparatus used in this study is essentially the same as the previous one as shown in Fig. 1-1. A detail description of the experimental apparatus and the procedure is given in the previous chapter.

2.1.3 Experimental Procedure

Measurement of ($H+L_2+G$) curve:

A small amount of H_2O was added to the pure Xe gas and liquid in equilibrium. After observing the boundary between the gas and liquid phases in the presence of hydrate phase in equilibrium, the equilibrium temperature and pressure were measured. The ($H+L_2+G$) curve lies slightly below the saturated vapor-pressure curve of pure Xe fluid. When the gas and liquid phases were critically identical in the presence of hydrate phase, such state was regarded as the critical end point($H+L_2=G$). The ($H+L_2+G$) curve terminates at the critical end point.

Measurement of ($H+L_1+G$) curve:

The three-phase coexisting curve($H+L_1+G$) originates from the quadruple point of $Q_1(H+S_1+L_1+G)$. The curve having no additional quadruple point $Q_2(H+L_1+L_2+G)$ exhibits the characteristic "S-shape" in the *p-T* diagram in a temperature range from 290 to 320 K and a pressure range up to 70 MPa.

The equilibrium pressure was measured with a pressure gage(Valcom VPRT) to an accuracy of ± 0.01 MPa and the temperature was measured within an accuracy of ± 0.02 K using a thermistor probe calibrated by a Pt resistance thermometer (Takara D-641).

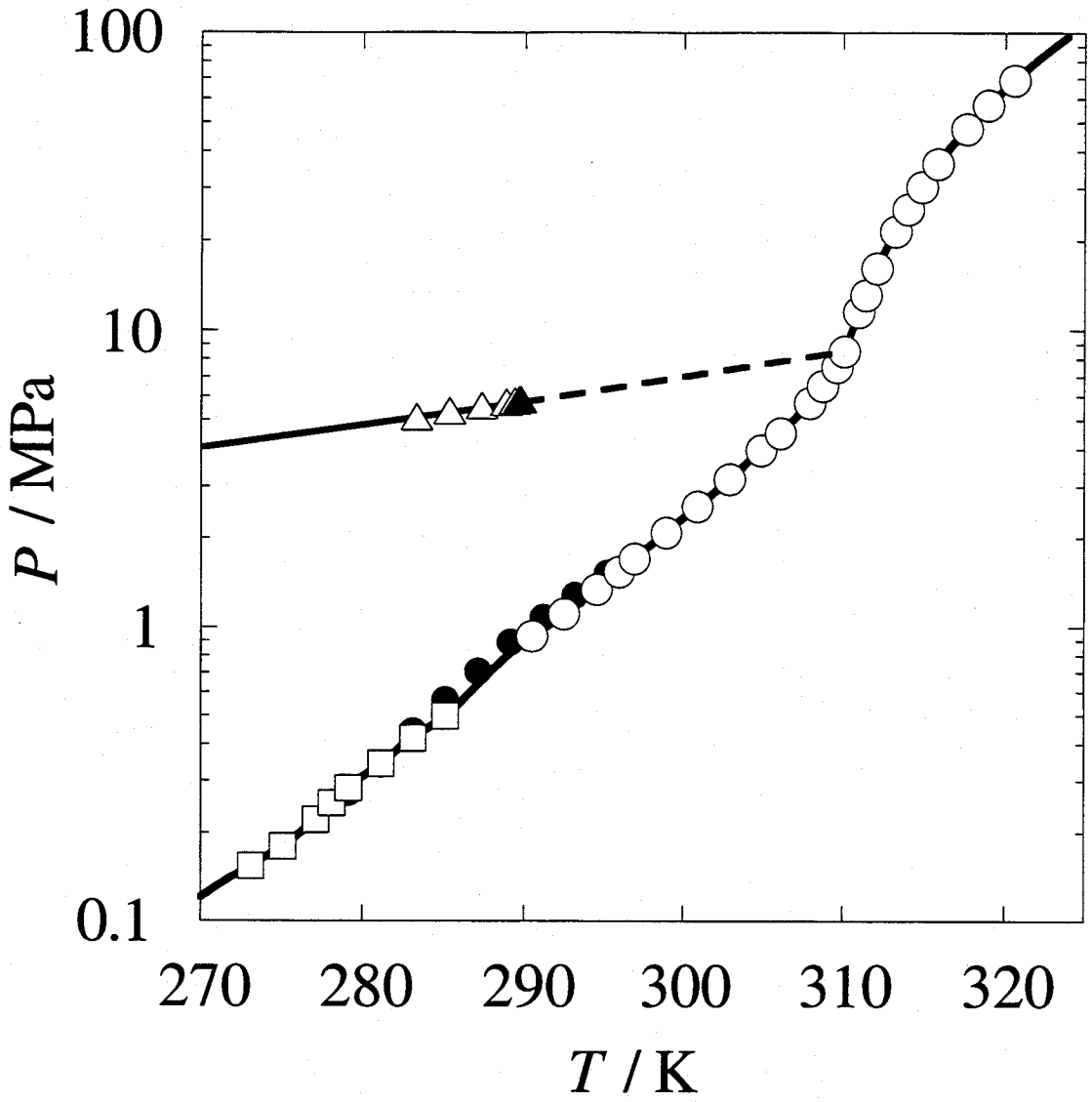

Fig. 2-1 Three-phase coexisting curves of the Xe hydrate system: O, ($H+L_1+G$ or F) in the present study; Δ, ($H+L_2+G$) in the present study; ▲, critical end point ($H+L_2=G$); ●, Balla-Achs and Berecz(1983); □, Ewing and Ionescu(1974).

2.2 Results and Discussion

The experimental pressure-temperature relations of the phase boundaries for the Xe hydrate system investigated in this study are listed in **Table 2-1** and shown in **Fig. 2-1**. The ($H+L_2+G$) curve lies slightly below the saturated vapor-pressure curve of Xe fluid and terminates at the critical end point($H+L_2=G$) of 289.76 K and 5.86 MPa, that is close to the Xe critical point of 289.7 K and 5.84 MPa. As the Xe system has the critical end point of ($H+L_2=G$), the system is identified as belonging to the type-q_1 diagram.

Table 2-1 Three-phase coexisting curves of the xenon hydrate system

T / K	P / MPa	T / K	P / MPa
$H+L_1+F_2$		$H+L_2+G$	
290.46	0.93	283.36	5.14
292.47	1.11	285.37	5.36
294.50	1.34	287.37	5.58
295.91	1.54	288.85	5.75
296.91	1.71	289.36	5.81
298.92	2.09	289.66	5.85
300.92	2.56	Critical end point	
302.92	3.16	289.76	5.86
304.90	3.96		
306.13	4.52		
307.93	5.71		
308.76	6.51		
309.63	7.56		
310.09	8.51		
310.99	11.56		
311.40	13.10		
312.11	16.18		
313.23	21.53		
314.02	25.58		
314.87	30.36		
315.84	36.23		
317.60	47.40		
318.96	56.93		
320.56	69.02		

The (H+L_1+G) curve that originated from the quadruple point Q_1 was investigated (Ewing and Ionescu, 1974) at the temperature of up to 285 K and at a pressure up to 0.5 MPa. When the (H+L_1+G) curve obtained in the present study is extrapolated to the low-pressure region, both the curves agree well. Balla-Achs and Berecz(1983) presented the (H+L_1+G) curve in a considerably high-pressure region of up to 1.5 MPa. However, their curve shifts slightly towards the higher pressure side as shown in Fig. 2-1. They also claimed that the Xe hydrate system belongs to type-q_2 diagram having the quadruple point of Q_2(H+L_1+L_2+G).

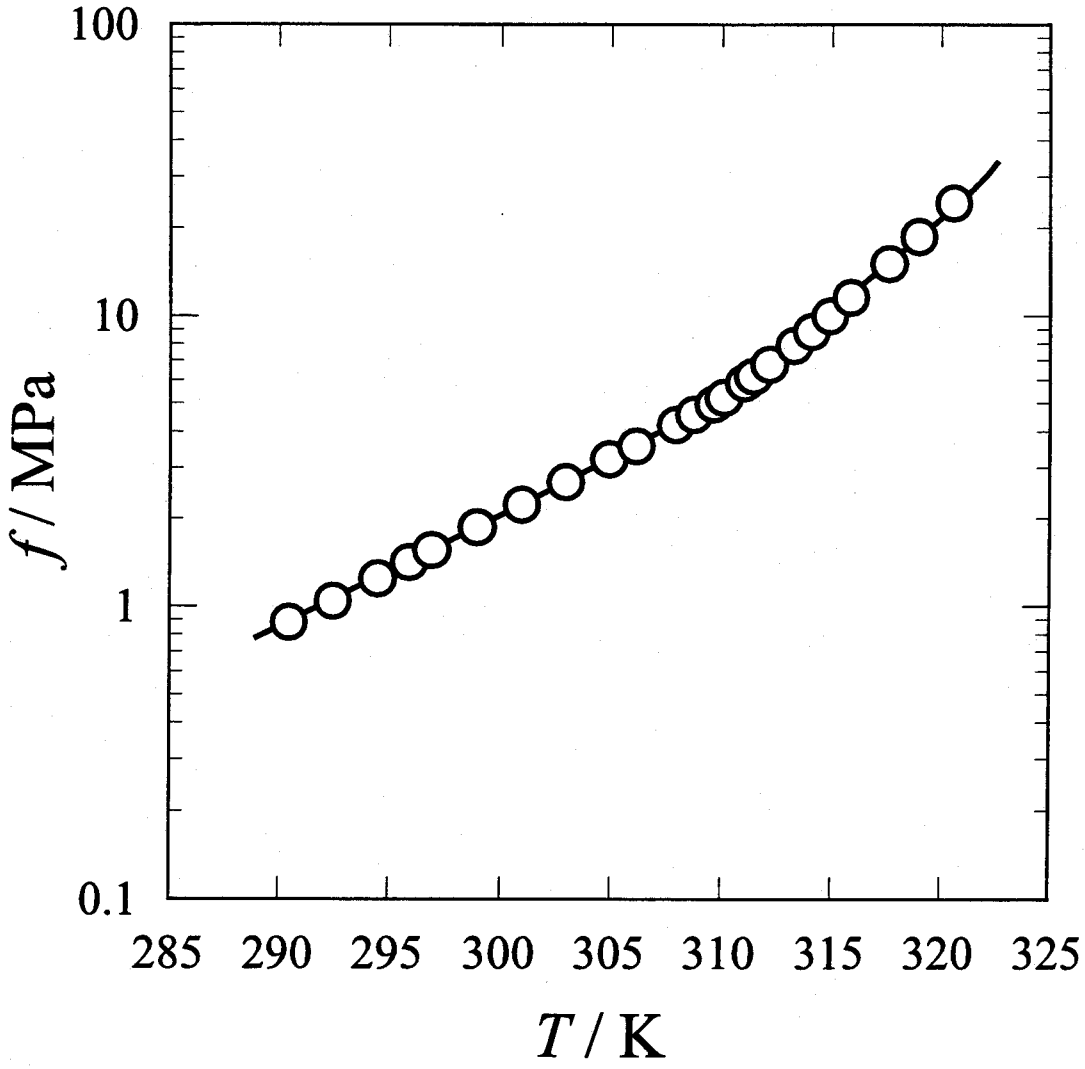

Fig. 2-2 Fugacity-temperature projection of (H+L_1+G) curve of the Xe hydrate system

The equilibrium curve in the high-pressure region shows the characteristic "S-shape" in the pressure-temperature projection as shown in Fig. 2-1. It seems as if there would be a quadruple point Q_2(H+L_1+L_2+G) where the broken line of the extrapolated (H+L_2+G) curve intersects the (H+L_1+G) curve. In fact, the slope of the (H+L_1+G) curve changes dramatically at the hypothetical quadruple point. Such curious behavior has been considered as the characteristic one appeared in the hydrate structural change (Balla-Achs and Berecz, 1983). On the other hand, Bansal *et al.*(1993) suggest that the S-shaped slope change might be caused by the characteristic *p-v-T* relation around the critical point. In the same opinion, we consider that the S-shaped equilibrium curve is a distinctive feature for the gas hydrate system where the critical end point (H+L_2=G) gets close to the (H+L_1+G) curve. Around the critical end point and slightly higher temperature region, anomalous critical phenomena are, in substance, caused by the relation of $(\partial p/\partial v)_T$ ~0 and then the fugacity coefficient of guest component suddenly decreases. The (H+L_1+G) curve described in the fugacity(f) - temperature(T) projection instead of the *p-T* projection is shown in **Fig. 2-2**. For calculating the fugacity, the Lewis fugacity rule is applicable to the xenon in the gas phase as the mole fraction is almost unity in these experimental conditions. The fugacity coefficient of pure xenon is calculated from Lee-Kesler equation of state (Reid *et al.*, 1986). The (H+L_1+G) curve described in *f-T* projection becomes a smooth curve which increases monotonically with the temperature.

The slope of $(dp/dT)_{equil.}$ was calculated at each data point on the three-phase equilibrium curve. From the combination of $(dp/dT)_{equil.}$ and molar volume of Xe hydrate, water and compressed Xe fluid, we can obtain the overall enthalpy change ΔH_{hyd} by using the Clausius-Clapeyron equation:

$$\left(\frac{dp}{dT}\right)_{equil.} = \frac{\Delta H_{hyd}}{\Delta v_{hyd} T} \qquad (2\text{-}1)$$

The total volume change Δv_{hyd} is defined by Eq. (2):

$$\Delta v_{hyd} = v_{Xe}^{F} + \lambda \cdot v_{H_2O}^{L} - v^{H} \qquad (2\text{-}2)$$

where v^{H} was calculated from the lattice constant of 1.20 nm (von Stackelberg, 1949) and v_{Xe}^{F} was obtained from the Lee-Kesler equation of state (Reid *et al.*, 1986). The hydration number λ was assumed to be 5.75(from the assumption of the ideal hydrate).

The ΔH_{hyd} at each data point is plotted in **Fig. 2-3**. It becomes an almost straight line and the average value of ΔH_{hyd}=65 kJ/mol shows a good agreement with the previous value of 64.8 kJ/mol (Ewing and Ionescu, 1974).

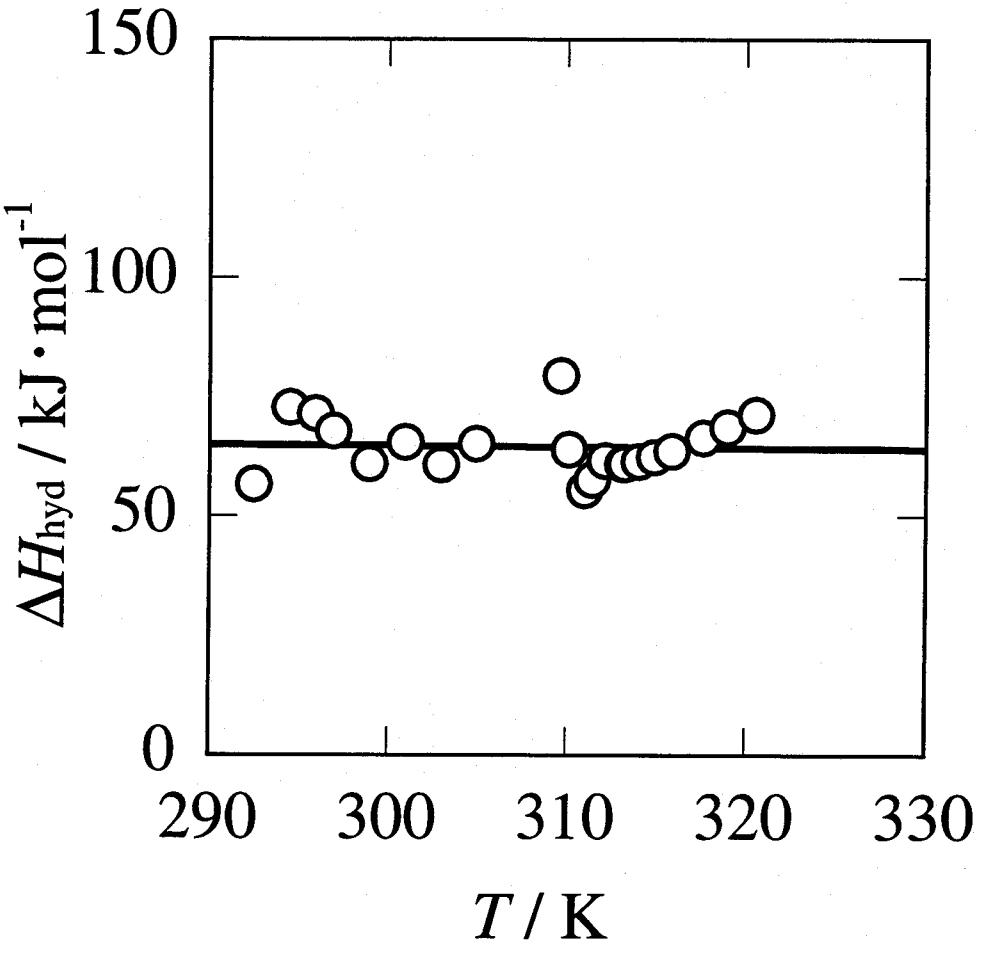

Fig. 2-3 Enthalpy change of the Xe hydrate formation

Summary

The three-phase coexisting curves of ($H+L_2+G$) and ($H+L_1+G$) for the Xe hydrate system have been determined in the temperature range from 290 to 320 K and pressure range up to 70 MPa. The invariant critical end point($H+L_2=G$) is located at 289.76 K and 5.86 MPa as the terminal point of ($H+L_2+G$) curve. The three-phase coexisting curve of ($H+L_1+G$) shows the characteristic "S-shape" curve in the *p-T* projection.

The existence of critical end point of ($H+L_2=G$) reveals that the Xe hydrate system belongs to the category q_1 which does not have additional quadruple point of ($H+L_1+L_2+G$). The Xe hydrate system is expected to be the border system of the type-q_1 in a series of critical temperatures of the guest molecules.

Nomenclature

f	=	fugacity	[Pa]
H	=	enthalpy	[J/mol]
p	=	pressure	[Pa]
T	=	temperature	[K]
v	=	molar volume	[m^3/mol]

< Greek >

λ	=	hydration number	[-]

<Symbols>

F	=	fluid phase
G	=	gas phase
H	=	hydrate phase
L	=	liquid phase
S	=	Solid phase

<Subscripts>

1	=	host component(water)
2	=	guest component(Xe)
hyd	=	hydration

Literature Cited

Balla-Achs, M. and E. Berecz, Gas Hydrate, Studies in Inorganic Chemistry 4, Elsevier, Amsterdam, 1983, pp176-182

Bansal, V., R. L. Christiansen and E. D. Sloan Jr., "Influence of Guest Vapor-Liquid Critical Point on Hydrate Formation Conditions," *AIChE Journal*, **39**, 1735-1737(1993)

Ewing, G. J. and L. G. Ionescu, "Dissociation Pressure and Other Thermodynamic Properties of Xenon-Water Clathrate," *J. Chem. Eng. Data*, **19**, 367-369 (1974)

Reid, R. C., J. M. Prausnitz and B. E. Poling, The properties of Gases & Liquids, 4th ed., p.47-49, McGraw-Hill Book Company, New York, USA (1986)

von Stackelberg, M., "Feste Gashydrate," *Naturwissenschaften*, **36**, 327-333 (1949)

Chapter III

Thermodynamical Stability Boundaries and Small Hydrate-cage Occupancy for the Ethylene Hydrate System

Abstract

Thermodynamical stability boundaries of ethylene hydrate system were investigated in a temperature range from 279 to 328 K and pressure range up to 465 MPa. The three-phase coexisting curve of the ethylene hydrate + saturated water + saturated fluid ethylene shows the characteristic "S-shape" behavior in the pressure-temperature projection. From the fugacity-temperature projection, it can be concluded that such curious behavior is caused by the anomalous critical phenomena. The laser Raman microprobe spectroscopic analysis reveals that the stretching and bending vibration energies of the ethylene entrapped into hydrate cage hold two different conditions. It has been argued that ethylene only occupies the large cage of structure-I. However, based on the double peaks from the Raman scattering on ethylene hydrate crystals, we give direct evidence that, in spite of ethylene's large van der Waals diameter, it also occupies the small cage.

Introduction

The four-phase coexisting point $Q_2(H+L_1+L_2+G)$ plays an important role in distinguishing the phase diagram of gas hydrate systems. The symbols H, G, L_1 and L_2 stand for the gas hydrate phase, the gas phase, the saturated liquid water phase and the saturated guest liquid phase. It is well-known that the temperatures of Q_2 for the trifluoromethane (Chapter I), carbon dioxide (Ohgaki and Hamanaka, 1995) and ethane (Morita *et al.*, 2000) hydrate systems locate at 280-295 K. Therefore, it is very interesting to make clear the phase behavior of gas hydrate systems where the guest species have the critical point in this temperature range. In the present study, ethylene is adopted as the guest molecule because the critical

temperature of ethylene is 282.4 K.

According to the literature (Berecz and Balla-Achs, 1983), the three-phase coexisting curve($H+L_1+F_2$) of ethylene hydrate system showed the behavior as if it had the four-phase coexisting point. Also, Bansal *et al.*(1993) reported such curious phase-behavior for the ethylene and xenon hydrate systems. Berecz and Balla-Achs(1983) claimed that such S-shaped stability boundary was due to the structural change of the hydrate crystal, on the other hand, Bansal *et al.*(1993) explained that it is some interesting phase-behavior close to the critical point of the guest fluid.

It is a matter of common knowledge that gas hydrates for the small guest molecules, as the xenon, methane, carbon dioxide, ethane and ethylene, configure to the unit cell structure-I. The structure-I consists of two small cages(S-cages) and six middle cages(M-cages). It has ever been believed that the ethane (0.53 nm in diameter) and ethylene (0.55 nm) are unable to occupy the S-cage(0.51 nm) because of its large van der Waals diameter, that is, such large guest can occupy only the M-cage(0.58 nm) to stabilize the structure-I lattice cell in the presence of vacant S-cages (Sloan, Jr., 1990).

However, Morita *et al.*(2000) reported that the ethane molecule can occupy the S-cage as well as M-cage from the double peaks of the C-C stretching vibration mode by means of the Raman spectroscopy, that is, they claimed that the guest molecule, whose van der Waals diameter is larger than the free void in the S-cage, can occupy the S-cage. Therefore, it is very interesting to investigate the possibility of the S-cage occupancy for ethylene, which has larger van der Waals diameter than ethane.

In the present study, the thermodynamical stability boundaries for the ethylene hydrate system have been determined by straightforward visual observation in a temperature range from 279 to 329 K and pressure range up to 465 MPa. The reason why such curious phase-behavior appears has been discussed briefly. In addition, the intramolecular vibration mode of the ethylene and the intermolecular vibration between the water molecules in the hydrate lattice were measured *in situ* by Raman microprobe spectroscopy. The pressure-dependence of each Raman active vibration mode was analyzed.

3.1 Experimental

3.1.1 Material

Research grade ethylene of purity 99.5 mol% was obtained from Takachiho Trading Co., Ltd, and used without further purification. The distilled water was obtained from Yashima Pure Chemicals Co., Ltd..

3.1.2 Experimental Apparatus

The experimental apparatus used in this study is essentially the same to the previous one (Nakano *et al.*, 1998). It was designed and manufactured to prepare single crystals of gas hydrates and moreover to perform *in situ* laser Raman spectroscopic analysis. It consists of several parts; a high-pressure cell having sapphire windows, a mixing ball operated by a vibrator, a high-pressure pump for supplying and/or pressurizing the samples, an intensifier, pressure gages, temperature control systems, and a charge-coupled device(CCD) camera and a laser Raman microprobe spectrometer.

For more accurate measurement, we used two different pressure gages according as the working pressure (up to 75 MPa: the pressure gage(Valcom VPRT) calibrated by RUSKA quartz Bourdon tube gage within an accuracy of ± 0.01 MPa, above 75 MPa: the pressure transducer(NMB STD-5000K) and digital peak holder(NMB CSD-819) within an accuracy of ±1 MPa).

The high-pressure optical cell was made of heat-treatment stainless steel(SUS 630). The schematic illustration of its cross-sectional view is shown in **Fig. 3-1**. The cell had inner volume of approximately 0.2 cm^3 and the maximum working pressure was about 500 MPa. A pair sapphire windows(their thickness was 5.5 mm.) was set on both the upper and lower sides of the inner volume. For reforming the lattice-defect of sapphire, the upper optical sapphire was Hot-Isostatic-Pressed at about 2100 K and 100 MPa by Kobe Steel Ltd. and had the surface of crystal face (0001). Each window was sealed with a packing made of Teflon type material. The depth and diameter of the inner volume, that was enveloped in both windows, were 4.5 and 7 mm, respectively. A ruby ball of 2 mm in diameter was enclosed with the inner space to agitate the system by

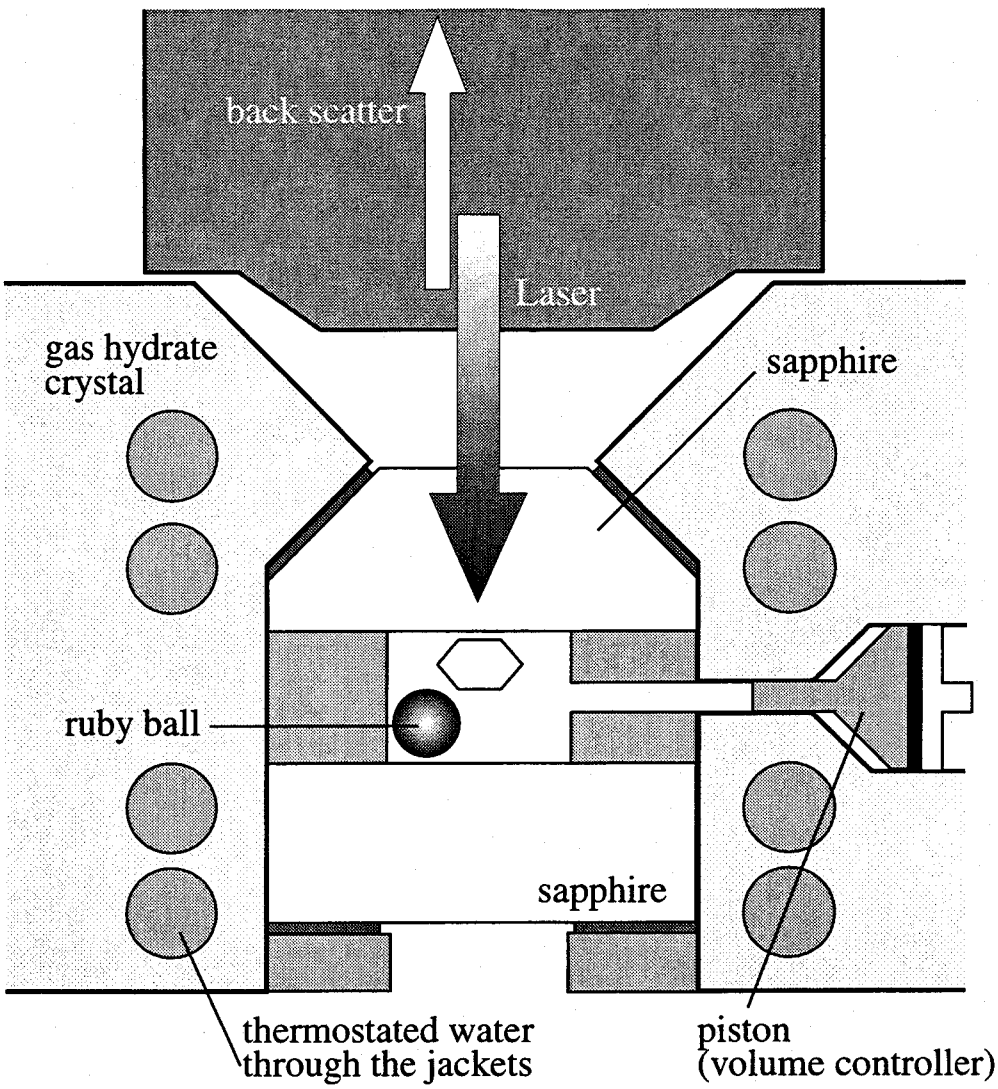

Fig. 3-1 Schematic diagram of the high-pressure optical cell in the sectional direction

vibration from outside. The contents were pressurized without changing the total amount of substances by use of a volume controller attached to the cell. The sectional area ratio between the water as the pressure-increasing medium and sample sides was about 30:1.

The system temperature was controlled by the thermostated water circulating from a thermocontroller(EYELA NCB-3100) thorough the jacket in the cell. The equilibrium temperature was measured within an accuracy of ± 0.02 K using thermistor probe(Takara D-641) calibrated by a Pt resistance thermometer inserted into a hole of the cell wall.

The water was pressurized by means of a high-pressure pump (Nihon

Seimitsu Kagaku NP-S-252) up to 35 MPa, and further pressurization was performed by means of the intensifier whose sectional area ratio was about 20:1. The phase behavior was observed by a CCD camera through the sapphire window.

3.1.3 Experimental Procedure

The ethylene was introduced into the high-pressure cell pre-vaccumed. And then, the contents were pressurized up to a desired pressure by successively supplying water or by controlling the inner volume. After the formation of ethylene hydrate, the system temperature was gradually increased to establish the three-phase coexisting state. The phase behavior was observed by the CCD camera through the sapphire window.

The single crystal of ethylene hydrate in equilibrium was analyzed by *in situ* Raman spectroscopy by use of a laser Raman microprobe spectrometer with a multichannel CCD detector. The laser beam from the object lens was irradiated to the sample through the upper sapphire window. The back scatter of the opposite direction was taken in with the same lens. The argon ion laser beam (514.5 nm and 100 mW) condensed to 2 μm in spot diameter was irradiated to the sample from the object lens. The spectral resolution was about 1 cm^{-1}. The integration time was varied within the range 10 to 300 sec, depending on the intensity of light scattering.

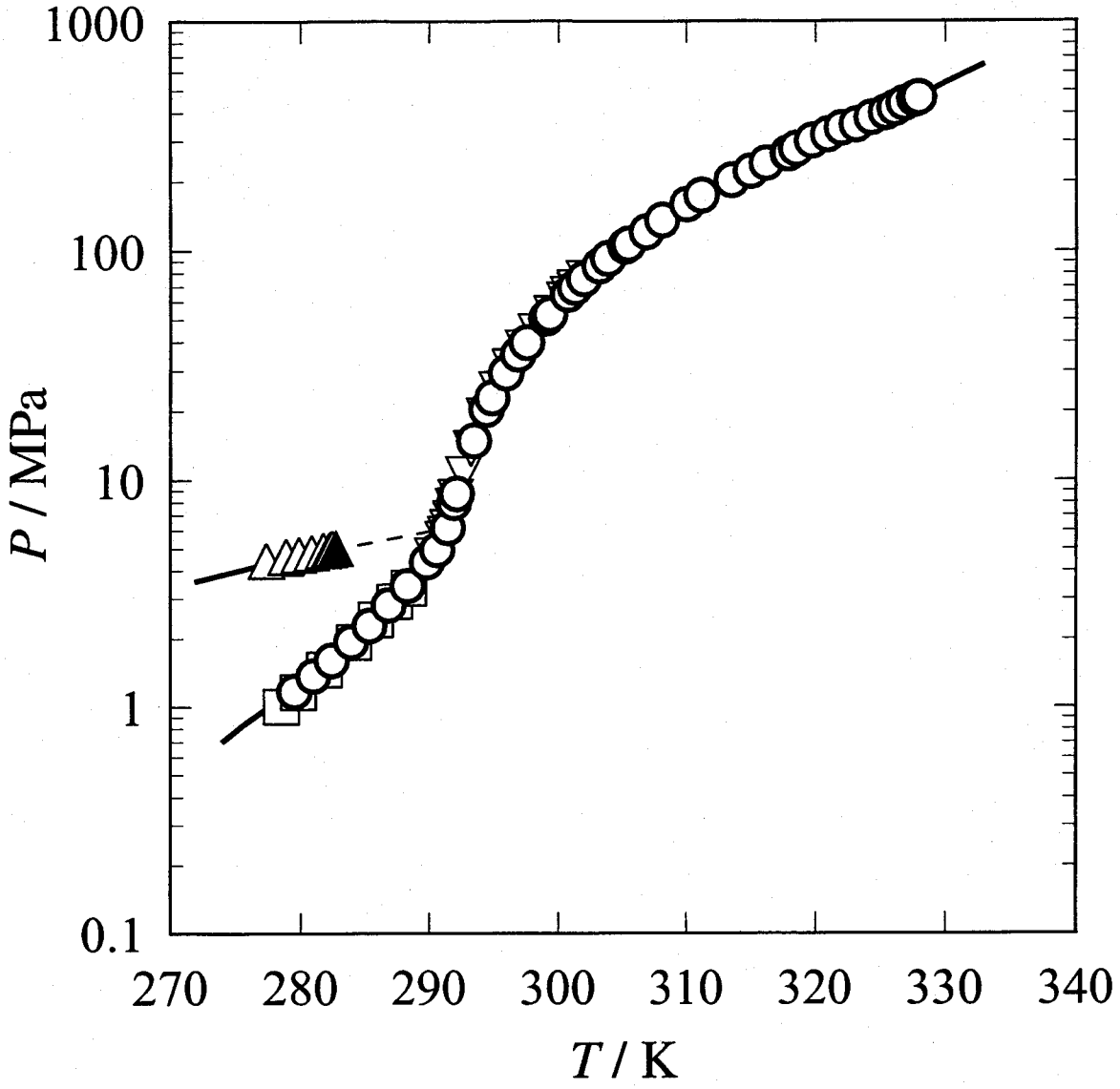

Fig. 3-2 Three-phase coexisting curves of the ethylene hydrate system: O, $H+L_1+F_2$ in the present study; □, Diepen and Scheffer(1959); ▽,van Cleeff and Diepen(1962); △, $H+L_2+G$ in the present study; ▲, critical end point($H+L_2=G$).

3.2 Results and Discussion

3.2.1 Three-phase coexisting curves of ($H+L_1+F_2$) and ($H+L_2+G$)

The experimental pressure-temperature relations of the phase boundaries for the ethylene hydrate system investigated in the present study are listed in **Table 3-1** and shown in **Fig. 3-2**. The data obtained agree well with the literature values (Diepen and Scheffer, 1959; van Cleeff and Diepen, 1962).

Table 3-1 Three-phase coexisting curves of ethylene hydrate system

T / K	P / MPa	T / K	P / MPa
	$H+L_1+F_2$		
279.54	1.17	310.04	159
281.00	1.37	311.17	174
282.42	1.61	313.49	203
283.94	1.94	314.97	222
285.36	2.29	316.17	240
286.86	2.82	317.90	265
288.33	3.42	318.50	278
289.84	4.36	319.72	301
290.64	4.93	320.97	320
291.46	6.16	322.05	342
291.94	7.93	323.23	354
292.15	8.69	324.39	380
293.48	14.86	325.51	399
294.45	20.38	326.19	416
294.89	22.89	326.90	437
295.96	29.35	327.69	457
296.89	35.39	328.01	465
297.56	39.77		
299.05	50.76	$H+L_2+G$	
299.32	52.70	277.40	4.42
300.72	64.43	278.87	4.58
301.27	69.04	279.88	4.71
301.97	75.41	280.86	4.81
303.16	86	281.76	4.91
303.84	92	282.24	4.96
305.16	104	282.47	5.02
305.42	107		
306.84	121	Critical end point	
308.08	136	282.73	5.03

The three-phase coexisting curve of ($H+L_2+G$) is about 0.1 MPa lower than the saturated vapor-pressure of ethylene. The pressure-discrepancy between them, in general, is very small because of very low water solubility in the guest liquid phase. The ($H+L_2+G$) curve terminates at the critical end point($H+L_2=G$), where the gas and liquid phases are critically identical in the presence of the hydrate phase. The critical end point is located at 282.73 K and 5.03 MPa, that is close to the pure ethylene critical point of 282.4 K and 5.04 MPa.

3.2.2 Specificity of the equilibrium curve of ($H+L_1+F_2$)

The equilibrium curve of ($H+L_1+F_2$) shows the characteristic "S-shape" in the pressure-temperature projection as shown in Fig. 3-2. It seems as if there would exist the quadruple point at the cross point of the extrapolated ($H+L_2+G$) curve and the ($H+L_1+F_2$) curve. In fact, the slope of the ($H+L_1+F_2$) curve changes dramatically at the point.

It had ever been believed that such slope change would be caused by the hydrate structural change. Bansal *et al.*(1993) suggest that the reason for the above S-shaped slope change may be due to the *p-v-T* relation around the critical point, not due to hydrate structural change. In the same opinion, we consider that the S-shaped equilibrium curve is a distinctive feature for the gas hydrate system where the critical end point ($H+L_2=G$), located near the pure gas-liquid critical point of the guest molecule, gets close to the ($H+L_1+F_2$) curve. Around the critical end point or slightly higher temperature region, some unusual phenomena are observed. Anomalous critical phenomena are, in substance, caused by the relation of $(\partial p/\partial v)_T \sim 0$, then the fugacity coefficient of fluid component suddenly decreases in this region. Therefore, the ($H+L_1+F_2$) curve described in the fugacity(f)-temperature(T) projection instead of the *p-T* projection is expected to become a smooth curve. The *f- T* curve in the interesting temperature-region is given in **Fig. 3-3**. For calculating the fugacity, the Lewis fugacity rule is applicable to the ethylene in the gas phase whose mole fraction is almost unity in these experimental conditions. The fugacity coefficient of pure ethylene is calculated from the equation recommended by IUPAC(Angus *et al.*, 1972). The ($H+L_1+F_2$) curve described in the *f-T* projection does not have the inflection point and the

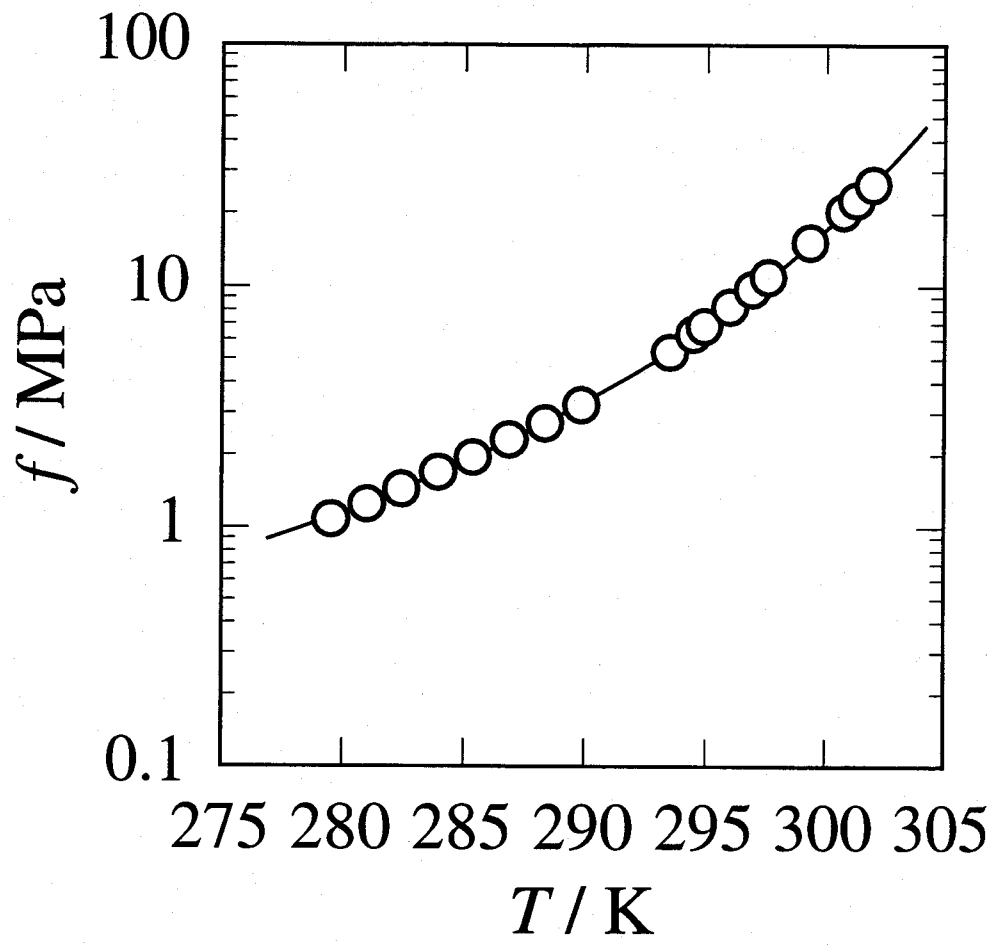

Fig. 3-3 Fugacity-temperature projection of ($H+L_1+F_2$) curve in the temperature range from 279 to 302 K.

fugacity increases monotonically with the temperature. The result reveals that the S-shaped curve (in the *p-T* projection) is caused by one of anomalous critical phenomena, not by solid phase transition.

3.2.3 Small-cage occupancy of ethylene molecule

The ethylene molecule has five Raman active vibration modes; C-H symmetric stretching (ca.. 3000 cm^{-1}), C=C stretching (ca.. 1600 cm^{-1}), H-C-H bending (ca.. 1350 cm^{-1}), C-H stretching (ca.. 3100 cm^{-1}) and H-C-C bending (ca.. 1250 cm^{-1}). The C-H symmetric, C=C stretching and H-C-H bending vibration modes were paid attention in the present study as the Raman peaks of the last two vibration modes were very weak. Typical Raman spectra of ethylene hydrate system measured at 95 MPa and 303.9 K under the three-phase coexisting are shown in **Fig. 3-4**. The spectrum for each Raman active vibration mode splits into a doublet in the ethylene hydrate phase, while a single peak is detected in both the saturated ethylene fluid and saturated water phases. For each vibration mode, the Raman shift of the larger peak in the hydrate crystal is very close to that of ethylene in the fluid and aqueous phases. To confirm what the larger peak in the hydrate crystal comes from, we prepared the two-phase coexisting state (ethylene hydrate + aqueous solution) in a similar pressure range. In the absence of the ethylene fluid phase, the split of Raman peaks is still detected from the ethylene hydrate crystal. From the above experiment, we can sustain that the double peaks in the hydrate crystal have no relation to the single peak in the fluid phase.

The split of the Raman peak in the hydrate phase indicates that the ethylene molecules are entrapped under the different energy conditions, that is, the ethylene molecules occupy both the S- and M-cages as well as the ethane molecule (Morita *et al.*, 2000). Considering the energy-level of the vibration, the larger peak (lower wave number) corresponds to ethylene entrapped in the M-cages, and the smaller one (higher wave number) to the S-cages. This is the first evidence for the S-cage occupancy of the ethylene molecule. As shown in Fig. 3-4, the difference between the C=C stretching energies of ethylene in the S- and M-cages is much smaller than that of the ethane C-C stretching ones (20 cm^{-1}). This implies that the C=C bond of ethylene is relatively tight compared with the ethane C-C bond.

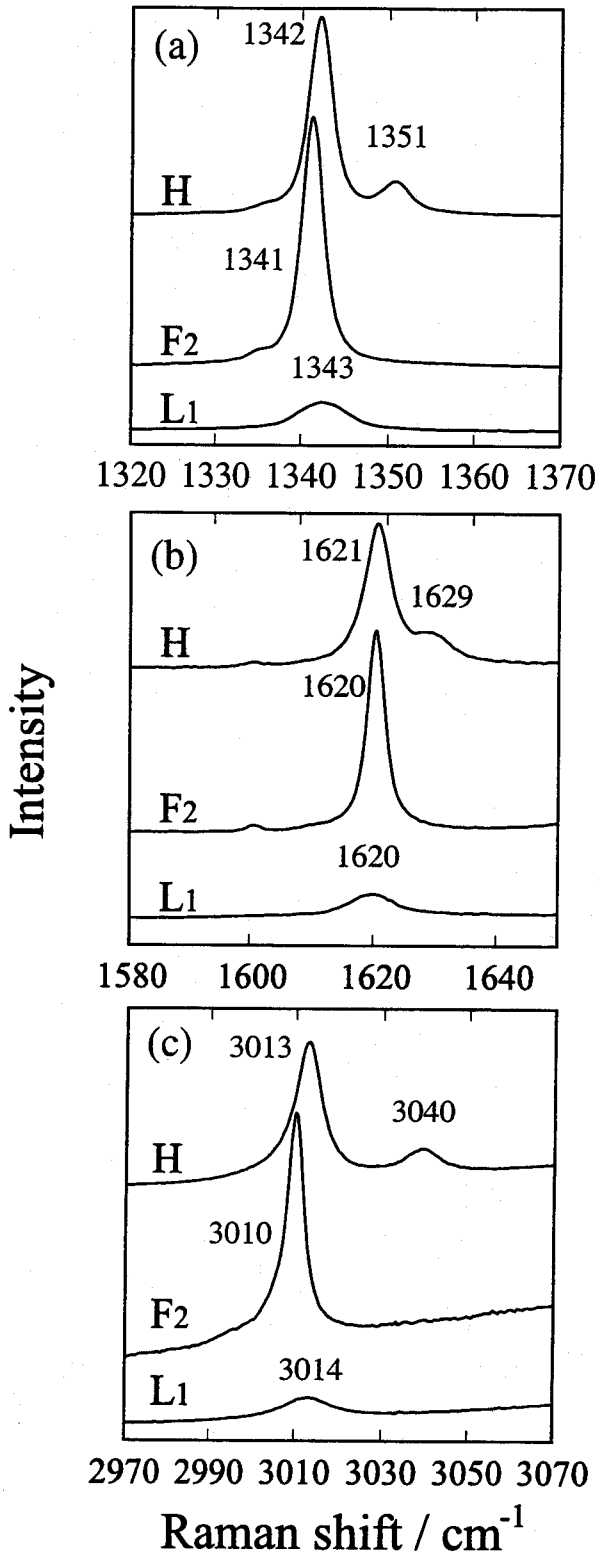

Fig. 3-4 Raman spectrum splits of the ethylene intramolecular vibrations at 95 MPa and 303.9 K on the three-phase coexisting curve. The vibration modes are as follows: (a), H-C-H bending, (b), C=C stretching, (c), C-H symmetric stretching. The symbols H, F_2, and L_1 stand for the gas hydrate phase, the ethylene fluid saturated with water, and the water phase saturated with ethylene, respectively.

3.2.4 Pressure-dependence of the intra- and inter-molecular vibration energies

The pressure-dependence of the Raman shift of the ethylene H-C-H bending vibration mode in a pressure range up to 500 MPa is shown in **Fig. 3-5-A**. The H-C-H bending vibration energies in the S-cage (key, O), aqueous solution (□) and the M-cage (△) decrease in that order. The first two of them

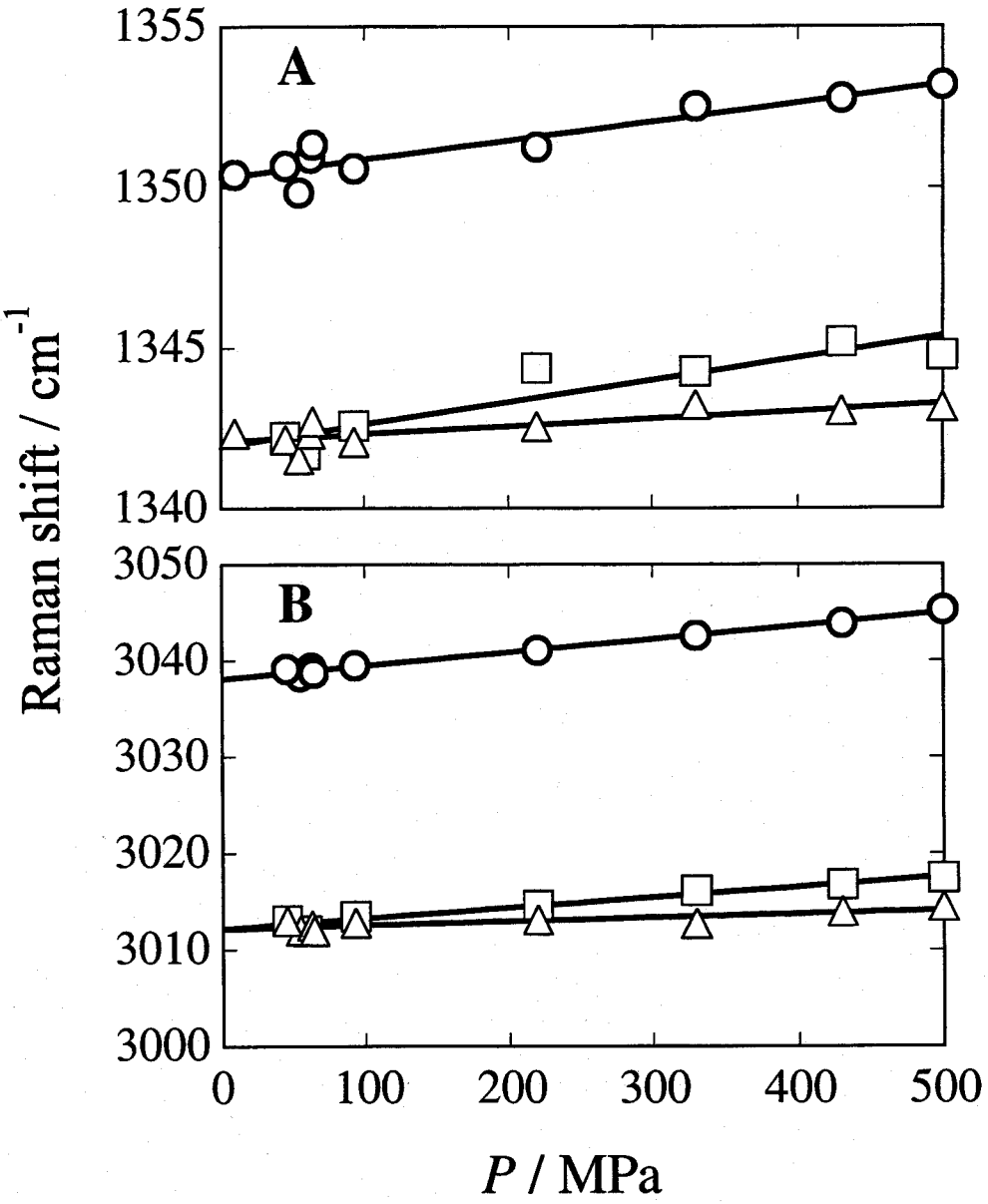

Fig. 3-5 Pressure dependence of the intramolecular vibration (**A**, H-C-H bending, **B**, C-H symmetric stretching) energies in the ethylene hydrate system. O, S-cage; △, M-cage; □, water phase

increase monotonically with pressure (0.6 cm^{-1}/100 MPa). They suggest that the hydrogen-bonded water cage shrinks gradually by pressurization and that the space around the ethylene molecule becomes smaller. On the other hand, the Raman shift in the M-cage is almost independent of pressure. It seems that the free volume in the M-cage is still large enough for the H-C-H bending vibration of ethylene in spite of the cage shrinkage.

The-pressure dependence of the ethylene C-H symmetric stretching vibration mode, being similar to that of the H-C-H bending vibration mode, is

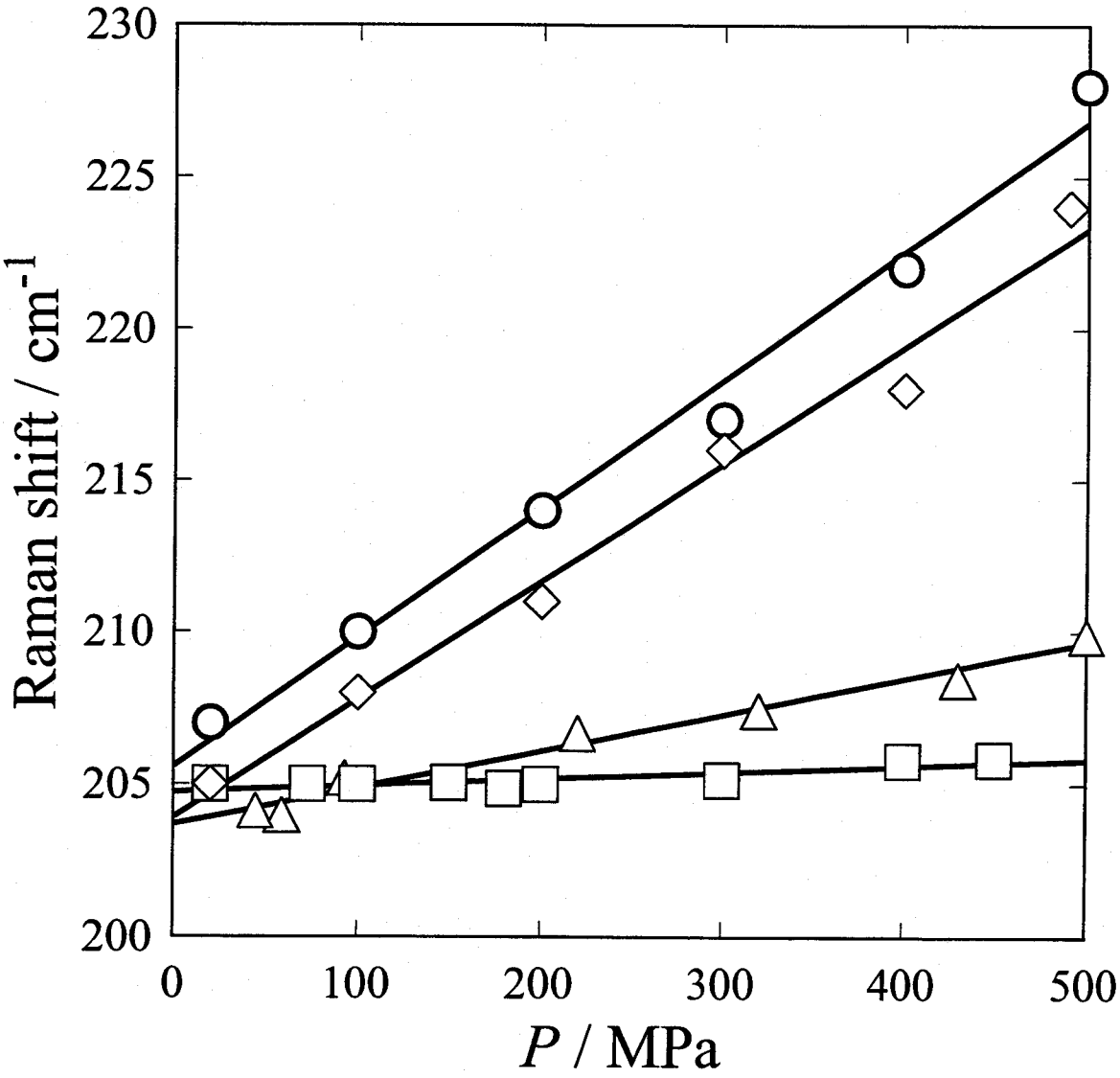

Fig. 3-6 Pressure dependence of the O-O vibration energy in the CO_2, methane, ethane, and ethylene hydrate systems: ◇, CO_2 hydrate; O, methane hydrate; □, ethane hydrate; △, ethylene hydrate.

shown in **Fig. 3-5-B**. The C-H symmetric stretching vibration energies in the S-cage and aqueous solution increase somewhat more strongly with pressure (1.5 cm^{-1}/100 MPa) and the vibration energy in the M-cage shows very weak pressure dependence (0.5 cm^{-1}/100 MPa). In addition, the pressure-dependence of the C=C stretching vibration, being not plotted in the figure, shows very similar behavior.

The Raman spectrum of intermolecular O-O vibration mode of water is observed around 200 cm^{-1} in the hydrate crystal. Needless to say, the O-O vibration energy is very important to investigate the elasticity of the hydrogen-bonded water cage. The pressure-dependence of the O-O vibration energy in the ethylene hydrate (△) is shown in **Fig. 3-6** accompanied with the results of CO_2(◇) (Nakano *et al.*, 1998), methane (○) (Nakano *et al.*, 1999) and ethane (□) (Morita *et al.*, 2000). The O-O vibration energy in the ethylene hydrate shows stronger pressure-dependence than that in the ethane hydrate, though it is not as strong as that in the methane and CO_2 hydrate systems. The stronger pressure-dependence would indicate the more shrinkage of the hydrogen-bonded cage or the larger free volume for the guest molecule. The free volume for the ethane molecule seems to be smaller than that for the ethylene molecule in hydrate cages. This implies that in spite of the largest van der Waals diameter of the ethylene molecule (0.55 nm) being larger than that of the ethane molecule (0.53 nm), the sequence of size might be reversed in other axes, which differ from the longest axis of the ethylene molecule because of ethylene having oblate shape. Therefore, the water cage of ethylene hydrate crystal may be deformed by the compression.

Summary

The three-phase coexisting curves of ($H+L_2+G$) and ($H+L_1+G$) for the ethylene hydrate system have been determined in the temperature range from 279 to 328 K and pressure range up to 465 MPa. The invariant critical end point ($H+L_2=G$) is located at 282.73 K and 5.03 MPa as the terminal point of ($H+L_2+G$) curve. The three-phase coexisting curve of ($H+L_1+G$) shows the characteristic "S-shape" curve in the *p-T* projection.

The Raman spectra of the intermolecular O-O vibration and the intramolecular H-C-H bending, C=C stretching and C-H symmetric stretching vibrations are observed in a pressure range up to 465 MPa. The intramolecular vibration energy in the S-cage shows clear pressure dependence. The intermolecular O-O vibration energy of the ethylene hydrate crystal shows stronger pressure dependence than that of the ethane hydrate crystal.

The important findings obtained from the Raman spectra measured in the present study are that the ethylene molecules can occupy both S- and M-cages of structure-I hydrate from the split of Raman peak in the hydrate phase.

Nomenclature

f	=	fugacity	[Pa]
p	=	pressure	[Pa]
T	=	temperature	[K]

<Symbols>

F = fluid phase
G = gas phase
H = hydrate phase
L = liquid phase
S = Solid phase

<Subscripts>

1 = host component(water)
2 = guest component(Ethylene)
hyd = hydration

Literature Cited

Angus, S., B. Armstrong, K. M. de Reuck, W. Featherstone and M. R. Gibson, *International Thermodynamic Tables of the Fluid States, Ethylene, 1972.* London: Butterworths. (1972)

Bansal, V., R. L. Christiansen and E. D. Sloan Jr., "Influence of guest vapor - liquid critical point on hydrate formation conditions," *AIChE Journal*, **39**, 1735-1737(1993)

Berecz, E. and M. Balla-Achs, *Gas Hydrates* (P. 207-208). Amsterdam: Elsevier. (1983)

Diepen, G. A. M. and F. E. C. Scheffer, "The ethylene-water system," *Rec. Trav. Chim.*, **69**, 593-603(1959)

Morita, K., S. Nakano and K. Ohgaki, "Structure and stability of ethane hydrate crystal," *Fluid Phase Equilibria*, **169**, 167-175(2000)

Nakano, S., M. Moritoki and K. Ohgaki, "High-pressure phase equilibrium and Raman microprobe spectroscopic studies on CO_2 hydrate system," *J. Chem. Eng. Data*, **43**, 807-810(1998)

Nakano, S., M. Moritoki and K. Ohgaki, "High-pressure phase equilibrium and Raman microprobe spectroscopic studies on the methane hydrate system," *J. Chem. Eng. Data*, **44**, 254-257(1999).

Ohgaki, K. and T. Hamanaka, "Phase-behavior of CO_2 hydrate-liquid CO_2-H_2O system at high pressure," *Kagaku Kogaku Ronbunshu*, **21**, 800-803(1995)

Sloan, E. D. Jr., *Clathrate Hydrates of Natural Gases*. (p. 46-49). New York: Marcel Dekker, Inc. (1990).

van Cleeff, A. and G. A. M. Diepen, "Ethylene hydrate at high pressures," *Rec. Trav. Chim.*, **81**, 425-429(1962)

Chapter IV

Pressure - Dependence of Small - Cage Occupancy for the Cyclopropane Hydrate System

Abstract

Laser Raman microspectroscopy and stability boundary observation for the cyclopropane hydrate system were investigated in a pressure range up to 460 MPa and temperature range from 278 to 320 K. The cyclopropane molecule is one of the largest guest species which build up the structure-I hydrate lattice. It has been argued that the cyclopropane hydrate lattice would become stable in the presence of the perfectly vacant small-cage. In the pressure range lower than 200 MPa, we can confirm the perfect vacancy of small hydrate cages. We have ascertained that the cyclopropane molecule is able to occupy the small hydrate cage in the pressure range higher than 200 MPa along with the three-phase coexisting curve. It becomes clear that the degree of small-cage occupancy increases in proportion to pressure without any phase transition in a pressure range up to 460 MPa.

Introduction

Thermodynamical stability of gas hydrates fundamentally depends on the temperature-pressure relation. The molecular size of guest species has direct effects upon the lattice structure and/or hydration number. Recent studies have shown that the hydrate structure is easily changeable, that is, the phase transition depends on not only the guest molecule but also the pressure-temperature conditions (Dyadin *et al.*, 1997). The structure change of hydrate lattice is also caused by adding a small amount of the third-component (Subramanian *et al.*, 2000a and 2000b, Ballard and Sloan Jr., 2000). The structure change from I to II in the methane hydrate system has been studied recently for the purpose of developing a new transportation method using natural-gas hydrate instead of liquid

natural-gas because of the advantage in the tanker volume and the heat consumption (Dyadin *et al.*, 1997).

The hydrate-cage occupancy by the guest molecule is also essential for the gas hydrate property. Two types of hydrate lattices, structure-I and structure-II, are well known. The guest molecular size physically dominates the hydrate-cage occupancy. It has been argued that some molecules such as ethane, ethylene, and cyclopropane are not able to occupy the S-cage because of their larger van der Waals diameter than the free volume of S-cage, that is, they would form the stable hydrate lattice in the presence of perfectly vacant S-cages (Sloan, Jr., 1990). However, we have presented elsewhere the direct evidence of S-cage occupancy by ethane (Morita *et al.*, 2000) and ethylene (Chapter III) from the Raman peak split of the intramolecular vibration mode in a pressure range from 20 to 500 MPa.

In the present study, the cyclopropane molecule having the largest van der Waals diameter among the guest molecules which form the hydrate structure-I is investigated. Four kinds of three-phase coexisting curves of cyclopropane hydrate phase(H) + aqueous solution(L_1) + gaseous phase(G), H + liquid cyclopropane phase(L_2) + G, L_1 + L_2 + G, and H + L_1 + L_2 have been observed straightforward including the quadruple point(H + L_1 + L_2 +G). The intramolecular symmetric ring-stretching vibration of cyclopropane and its pressure dependency in each phase are analyzed by using Raman microspectroscopy along with the three-phase coexisting curve (H + L_1 + L_2) in a pressure range from 100 to 460 MPa.

4.1 Experimental

The experimental apparatus used in this study is essentially the same as the previous one as shown in Fig. 3-1. A detail description of the experimental apparatus and the procedure is given in the previous chapter.

Research grade cyclopropane (purity 99.5 mol%) was obtained from Takachiho Trading and used without further purification. The distilled water was obtained from Yashima Pure Chemicals.

4.2 Results and discussion

4.2.1 Three-phase coexisting curves

The experimental pressure-temperature relations of the phase boundaries for the cyclopropane hydrate system investigated in this study are listed in **Table 4-1** and shown in **Fig. 4-1**. We have observed an intrinsic point of the quadruple point (H + L_1 + L_2 + G) at 289.46 K and 0.56 MPa, which are very close to the literature values of 289.56 K and 0.56 MPa (Hafemann & Miller, 1969). Four kinds of three-phase coexisting curves originated from the quadruple point have

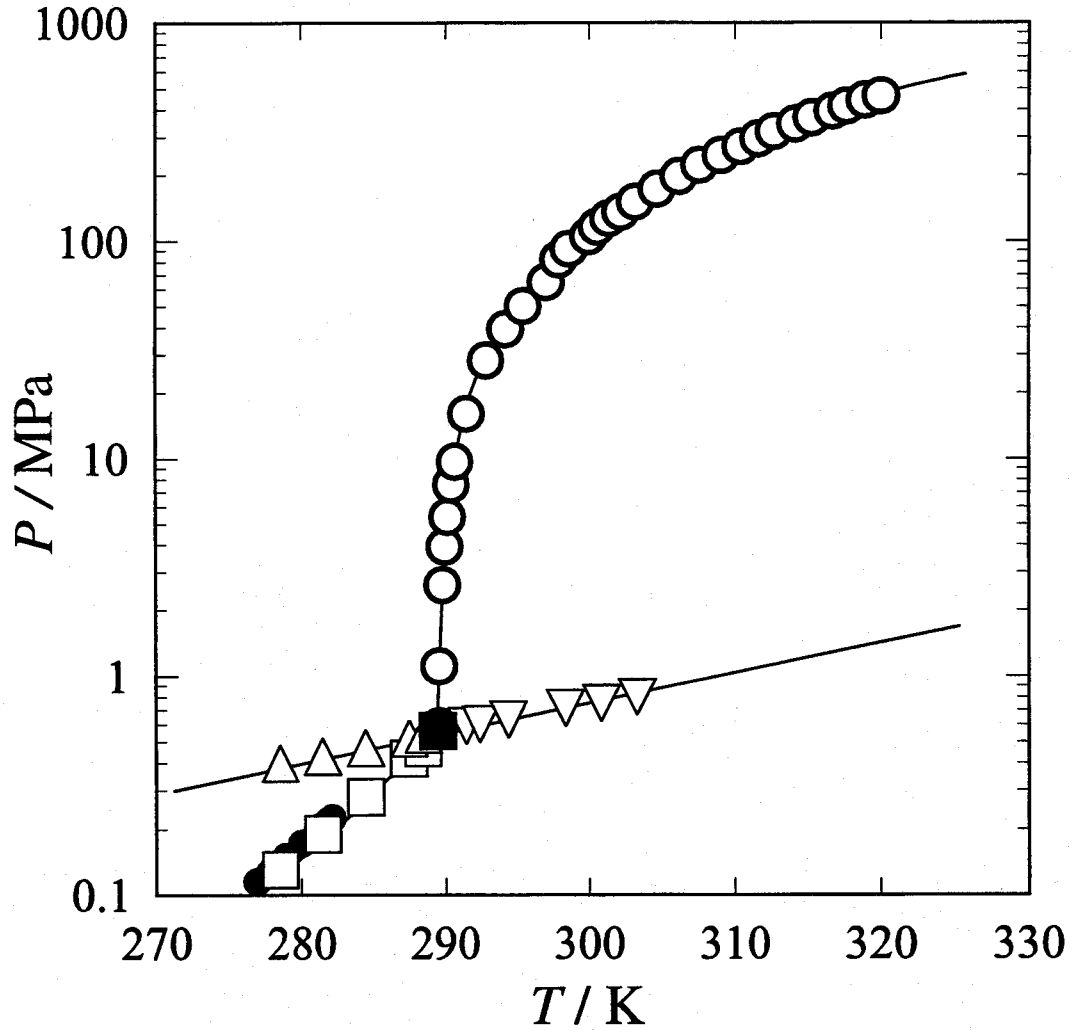

Fig. 4-1 Three-phase coexisting curves of the cyclopropane hydrate system: O, H+L_1+L_2 in the present study; □, H+L_1+G in the present study; ●, Hafemann and Miller(1969); △, H+L_2+G in the present study; ▽, L_1+L_2+G in the present study; ■, quadruple point

been measured. Majid & Davidson (1969) claimed from the slope change of the three-phase coexisting curve that the phase transition from structure-I to structure-II occurs in a temperature region from 257.15 to 274.65 K. As the present experimental equipment is not suitable for measuring phase equilibria at low temperature and pressure, the temperature range is not extended to such a low region. Therefore, the symbol H stands for the cyclopropane hydrate of structure-I in this chapter. The three phase coexisting (H + L_1 + G) curve agrees well with the literature (Hafemann & Miller, 1969). The (L_1 + L_2 + G) curve, lying just below the saturated vapor-pressure curve of pure cyclopropane fluid, terminates at the critical end point (L_1 + L_2 = G). The (L_1 + L_2 + G) and (H + L_2 + G) curves interconnect at the quadruple point. The three-phase coexisting (H + L_1 + L_2) curve originated from the quadruple point extends to the high pressure direction. The curve plotted in the T-ln P projection is bent laterally around 100 MPa. There is no phase transition (structure-I to structure-II) in the whole range in this study.

Table 4-1 Three-phase coexisting curves of cyclopropane hydrate system

T / K	P / MPa	T / K	P / MPa
$H+L_1+L_2$		$H+L_1+G$	
289.54	0.59	278.52	0.13
289.57	1.11	281.49	0.19
289.80	2.62	284.48	0.28
289.96	3.93	287.45	0.42
290.15	5.39	288.44	0.47
290.41	7.60		
290.67	9.67	$H+L_2+G$	
291.47	16.05	278.53	0.40
292.86	28.28	281.50	0.43
294.23	39.35	284.47	0.47
295.44	50.21	287.49	0.52
297.02	64.58	288.48	0.54
297.89	82	289.45	0.56
298.60	92		
299.95	105	L_1+L_2+G	
300.54	116	289.53	0.56
301.33	127	290.15	0.56
302.15	136	291.44	0.59
303.14	151	292.43	0.60
304.62	173	294.41	0.63
306.14	198	298.35	0.71
307.56	223	300.82	0.75
309.03	247	303.28	0.80
310.39	271		
311.61	295	Quadruple point	
312.69	318	289.46	0.56
314.17	344		
315.31	368		
316.73	394		
317.68	416		
318.93	443		
320.01	463		

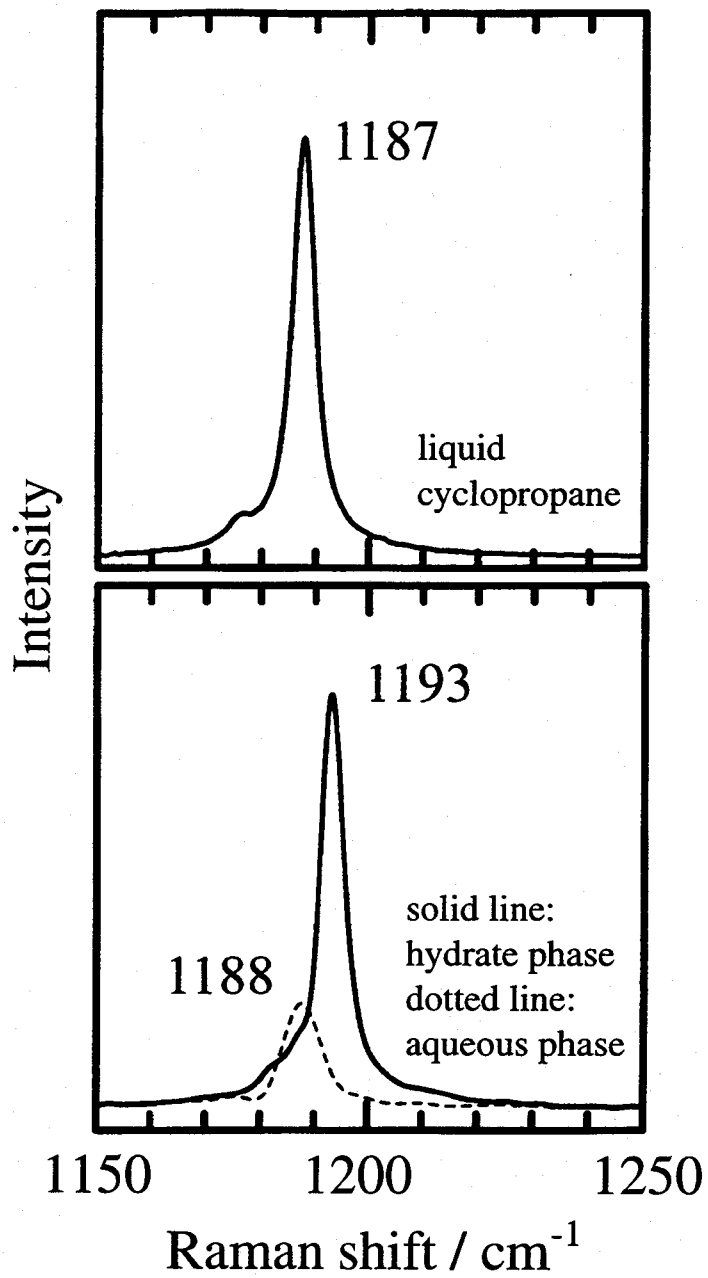

Fig. 4-2 Raman spectra of the symmetric ring-stretching vibration mode of cyclopropane molecule in the fluid cyclopropane, cyclopropane hydrate and aqueous phases at 100 MPa

4.2.2 *In situ* laser Raman microprobe spectroscopy

The cyclopropane molecule has several Raman active vibration modes. Only the symmetric ring-stretching vibration mode is paid attention in this study because other modes exhibit very broad Raman peaks. According to the literature (Tobin, 1971), the Raman peak for the symmetric ring-stretching vibration in the cyclopropane molecule is detected around 1200 cm^{-1}. Typical Raman spectra

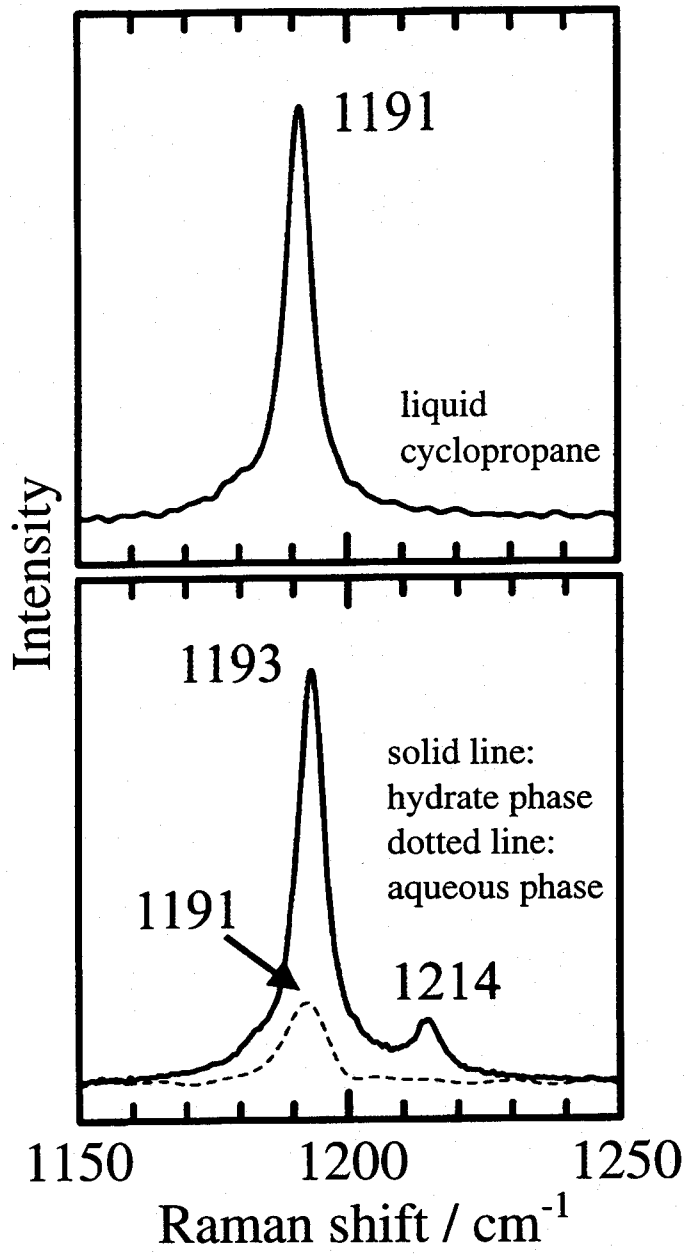

Fig. 4-3 Raman spectra of the symmetric ring-stretching vibration mode of cyclopropane molecule in the fluid cyclopropane, cyclopropane hydrate and aqueous phases at 460 MPa

detected for the cyclopropane hydrate system at 100 MPa are shown in **Fig. 4-2.** A single Raman peak is detected around 1190 cm^{-1} for the symmetric ring-stretching vibration in the cyclopropane hydrate phase as well as the aqueous solution and liquid cyclopropane phases in the pressure range lower than 200 MPa. This fact reveals that the cyclopropane molecule can occupy only the M-cage in the lower pressure region (< 200 MPa).

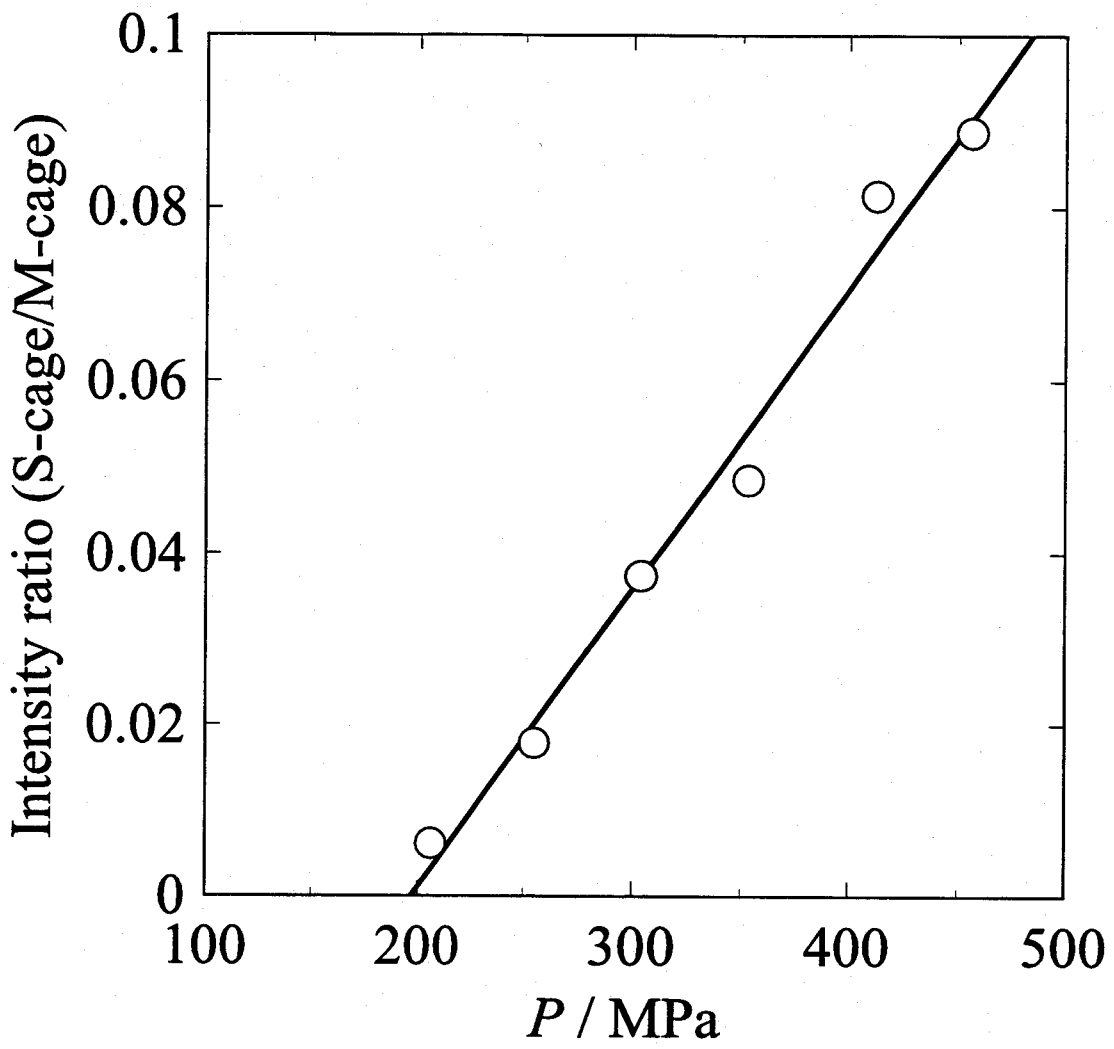

Fig. 4-4 Pressure effect on the relative Raman-peak intensity of cyclopropane molecules in S-cage to M-cage

As the pressure is raised, however, the double peaks in the cyclopropane hydrate phase are newly detected around 1210 cm^{-1} in addition to the Raman-peak around 1190 cm^{-1} as shown in **Fig. 4-3** (at 460 MPa). That is, the spectrum in the cyclopropane hydrate phase splits into a doublet in the higher pressure, while a single peak was detected in both the aqueous and liquid cyclopropane phases. These findings reveal that the cyclopropane molecule is able to be entrapped into both the S- and M-cages as well as the ethane (Morita *et al.*, 2000) and ethylene (Chapter III) molecules. The Raman-peak intensity of the cyclopropane molecules in S-cage becomes larger as the compression. The relative Raman-peak intensity of S-cage to M-cage versus pressure is shown in **Fig. 4-4**. The intensity ratio

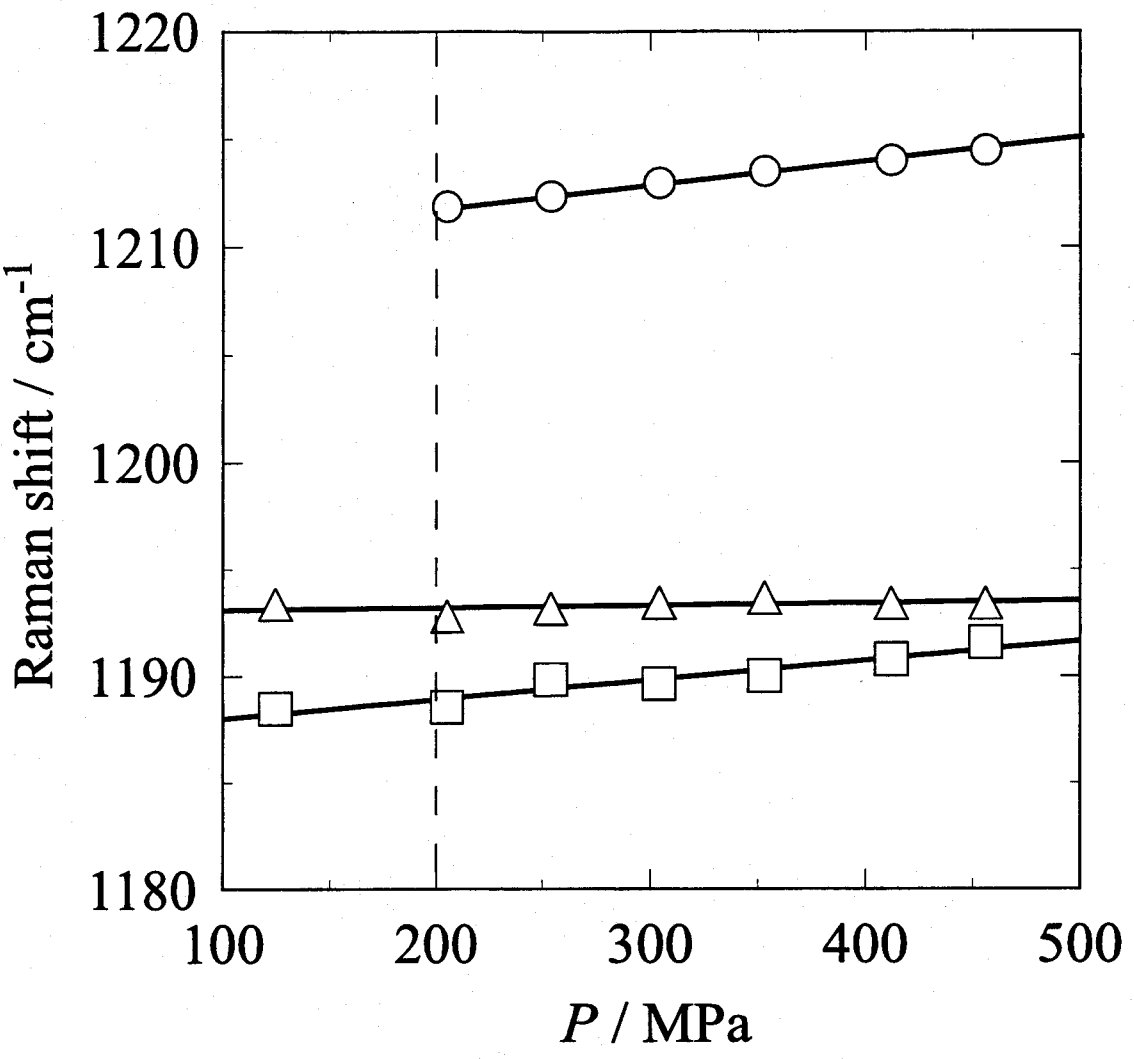

Fig. 4-5 Pressure effect on the ring-stretching vibration energies in cyclopropane hydrate system. O, S-cage; △, M-cage; □, water phase

($I_{S\text{-cage}}$ / $I_{M\text{-cage}}$) is linearly increased with pressure under the present experimental conditions. The intensity ratio becomes zero at 200 MPa, that is, the cyclopropane molecule is able to be entrapped into S-cage in the pressure range above 200 MPa while the S-cage is perfectly vacant in the lower pressure region.

4.2.3 Pressure - dependence of the intra- and inter-molecular vibration

The pressure effect on Raman shifts of the symmetric ring-stretching vibration mode of the cyclopropane molecule in a pressure range up to 460 MPa is shown in **Fig. 4-5**. The ring-stretching vibration energies in the S-cage of the

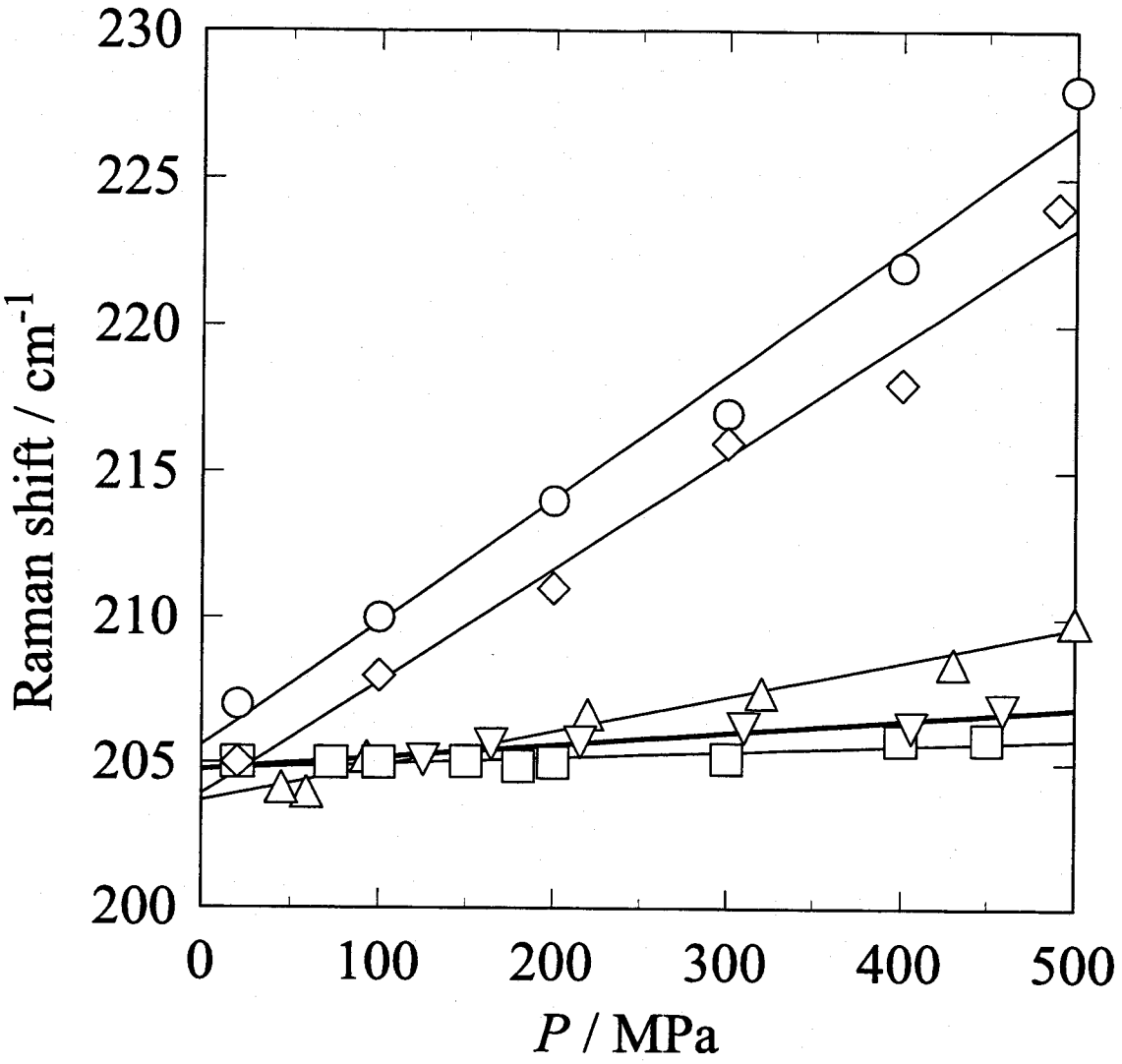

Fig. 4-6 Pressure effect on the O-O vibration energy in the cyclopropane, methane, CO_2, ethylene and ethane hydrate systems: ▽, cyclopropane hydrate; O, methane hydrate; ◇, CO_2 hydrate; △, ethylene hydrate; □, ethane hydrate.

cyclopropane hydrate phase and water phase increase monotonically with pressure (both of them are ~ 1 cm^{-1} / 100 MPa). Such pressure dependency is the characteristic behavior for guest species entrapped in the S-cage of structure-I hydrate. The space around the cyclopropane molecule in the S-cage would become smaller by pressurization. However, the Raman shift in the M-cage of the cyclopropane hydrate is almost independent of pressure. The pressure independency has been also presented for the methane (Nakano *et al.*, 1999), ethane (Morita *et al.*, 2000) and ethylene (Chapter III) molecules in the M-cage. It

would imply that the inner volume of M-cage is still enough for the guest molecule in this pressure range.

The Raman spectrum of intermolecular O-O vibration mode of water is observed around 205 cm^{-1} in the cyclopropane hydrate crystal. The pressure dependence of the O-O vibration energies in the cyclopropane hydrate is shown in **Fig. 4-6** accompanied with the results of CO_2, methane, ethane and ethylene hydrate systems. The O-O vibration shift exhibits the strong pressure dependence in the hydrate systems of methane and CO_2 which have somewhat small van der Waals diameter. The pressure dependence suggests that the hydrate cage constructed of water molecules shrinks gradually by pressurization. On the other hand, the O-O vibration shift is relatively independent of the pressure in the hydrate systems of ethane, ethylene and cyclopropane which have large van der Waals diameter. It means that the hydrate cages are not easily shrunk by pressurization.

Summary

Four kinds of three-phase coexisting curves and one intrinsic quadruple point (289.46 K, 0.56 MPa) for the cyclopropane hydrate system were measured up to 460 MPa by use of an optical cell with sapphire windows.

The single crystal of cyclopropane hydrate was analyzed *in situ* by use of laser Raman microprobe spectroscopy. The Raman spectra of the symmetric ring-stretching vibration of the cyclopropane molecule and the intermolecular O-O vibration were observed in a pressure range up to 460 MPa. The following findings are obtained.

1) The split of Raman spectra for the symmetric ring-stretching vibration in the cyclopropane hydrate crystal is detected in the high pressure range above 200 MPa, while a single peak is observed up to the pressure. This fact indicates that the cyclopropane molecule can occupy both the S- and M-cages of structure-I hydrate at least above 200 MPa.
2) The symmetric ring-stretching vibration energies of the cyclopropane molecule in the S-cage and the aqueous solution show similar pressure dependence, while the vibration energy in the M-cage is almost independent of pressure.
3) The intermolecular O-O vibration energy in the cyclopropane hydrate crystal is almost independent of pressure and this behavior is very similar to that of the ethane hydrate crystal.

Nomenclature

p	=	pressure	[Pa]
T	=	temperature	[K]
I	=	Raman intensity	

<Symbols>

G	=	gas phase
H	=	hydrate phase
L	=	liquid phase

<Subscripts>

1	=	host component(water)
2	=	guest component(cyclopropane)

Literature Cited

Ballard, A. L. and E. D. Sloan Jr., "Structural transitions in methane + ethane gas hydrates - Part II: modeling beyond incipient conditions," *Chem. Eng. Sci.*, **55**, 5773-5782(2000)

Dyadin, Y. A., E. G. Larionov, D. S. Mirinski, T. V. Mikina and L. I. Starostina, "Clathrate formation in the Ar-H_2O system under pressures up to 15000 bar," *Mendeleev Commun.*, 32-33(1997a)

Dyadin, Y. A., E. Y. Aladko and E. G. Larionov, "Decomposition of methane hydrates up to 15 kbar," *Mendeleev Commun.*, 34-35(1997b)

Hafemann, D. R. and S. L. Miller, "The clathrate hydrates of cyclopropane," *J. Phys. Chem.*, **73**, 1392-1397(1969)

Majid, Y. A., S. K. Garg and D. W. Davidson, "Dielectric and nuclear magnetic resonance properties of a clathrate hydrate of cyclopropane," *Can. J. Chem.*, **47**, 4697-4699(1969)

Morita, K., S. Nakano and K. Ohgaki, "Structure and stability of ethane hydrate crystal," *Fluid Phase Equilibria*, **169**, 167-175(2000)

Nakano, S., M. Moritoki and K. Ohgaki, "High-pressure phase equilibrium and Raman microprobe spectroscopic studies on the CO_2 hydrate system," *J. Chem. Eng. Data*, **43**, 807-810(1998)

Nakano, S., M. Moritoki and K. Ohgaki, "High-pressure phase equilibrium and Raman microprobe spectroscopic studies on the methane hydrate system," *J. Chem. Eng. Data*, **44**, 254-257(1999)

Sloan, Jr., E. D. *Clathrate Hydrates of Natural Gases*. (p.46-50). New York: Marcel Dekker, Inc. (1990)

Subramanian, S., R. A. Kini, S. F. Dec and E. D. Sloan, Jr., "Evidence of structure II hydrate formation from methane + ethane mixtures," *Chem. Eng. Sci.*, **55**, 1981-1999(2000a)

Subramanian, S., A. L. Ballard, R. A. Kini, S. F. Dec and E. D. Sloan, Jr., "Structural transitions in methane + ethane gas hydrates - Part I: upper transition point and applications," *Chem. Eng. Sci.*, **55**, 5763-5771(2000b)

Tobin, M. C., *Laser Raman Spectroscopy, Chemical Analysis*. 35, (p. 96). New York: John Wiley & Sons, Inc. (1971)

Chapter V

Hysteresis in Dissociation and Reformation of Methane Hydrate Crystal

Abstract

A methane hydrate crystal annealed at maximum pressure remembers the compression in the hydrate S-cage until the higher equilibrium temperature for maximum pressure is reached. The hydrate S-cage-like structure in the aqueous solution also remembers the compression until the so-called activation energy is given by heating. Therefore, the hydrate crystal compressed by the maximum pressure is reformed at the equilibrium temperature for the maximum pressure.

Introduction

We have previously reported pressure-dependence on the intermolecular and intramolecular vibration energies as well as the thermodynamical stability boundary of methane hydrate crystal in a pressure range up to 500 MPa (Nakano *et al.*, 1999). In measurement of the stability boundary, the greatest care had to be taken about the hysteresis-effect on the equilibrium temperature-pressure relation. In the present study, we examine by using a laser Raman microprobe spectrometer what the hysteresis is in the dissociation and reformation processes, and how long in the aqueous solution the residual energy is held.

Since the gas-hydrate field under the deep-ocean floor has become the object of attention as a potential unconventional energy resource (Kvenvolden, 1988; Ohgaki et al., 1994), studies on physical and chemical properties of methane hydrate crystal have been accelerated. It is, however, still unclear why the gas-hydrate crystal is easily reformed once the hydrate has been formed and dissociated, although there has been much speculation (Sloan, 1990). We also found out that a gas-hydrate crystal prepared at supersaturated pressures is able to

remain for quite a long time in the unstable region.

The interesting findings in our previous study (Nakano *et al.*, 1999) are summarized as follows: the Raman peak (around 200 cm^{-1}) of intermolecular O-O vibration of water is a peculiar spectrum of the gas-hydrate lattice; it shows strong pressure-dependence in the range from 100-500 MPa; the C-H stretching vibration peak (around 2900 cm^{-1}) of the methane molecule in the aqueous solution is similar to that of the methane molecule entrapped in the hydrate pentagonal dodecahedron cavity (S-cage) and both vibrations show considerable pressure-dependence; however, the C-H vibrations of the methane molecules in the hydrate tetrakaidecahedron cavity (M-cage) and in the water-saturated methane fluid are almost independent of pressure. Giving attention to pressure-dependence of each vibration, we examine the intrinsic nature of hysteresis in the dissociation and reformation of methane hydrate crystal by using a laser Raman microprobe spectrometer.

5.1 Experimental

5.1.1 Materials

Research grade methane (purity 99.95 %) was obtained from Takachiho Trading Co., Ltd. and used without further purification. The distilled water was obtained from Yashima Pure Chemicals Co., Ltd..

5.1.2 Phase behavior

The experimental strategy applied is schematically shown in **Fig. 5-1**. Following the direction of the arrow, the system temperature and pressure were changed gradually. The phase behavior was observed by a camera through the cell window during the entire process. Details of the experimental apparatus are given elsewhere (Nakano *et al.*, 1999). The methane hydrate crystal was first prepared at point A (290 K, 20 MPa in equilibrium). The system temperature and pressure were increased gradually along with the stability boundary curve where the methane hydrate + saturated water + saturated methane fluid are in equilibrium. After the Raman spectroscopic analysis at point B (320 K, 500 MPa in

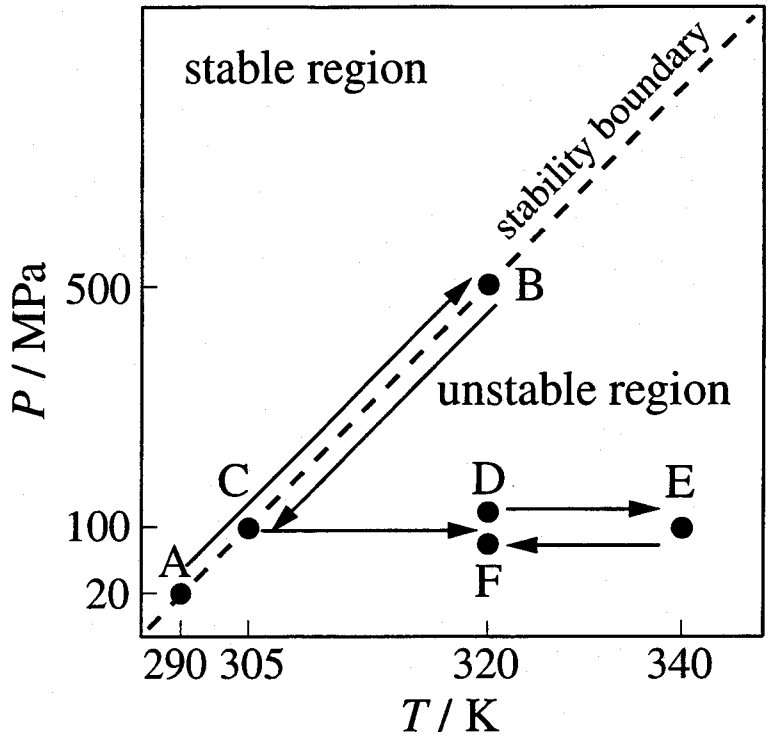

Fig. 5-1 Experimental strategy of hysteresis measurement

equilibrium), the contents were depressurized and cooled to point C (305 K, 100 MPa) and held for 12 hours. Maintaining the system pressure, the temperature was increased until the hydrate crystal was dissociated at point D (~320 K, 100 MPa). After that, the fluid mixture of methane and water was heated and held for three days at point E (340 K, 100 MPa). During the cooling process from E to C, the hydrate crystal was reformed at point F (close to D). The temperature of D and F corresponds to that of the maximum pressure. Heating and cooling were performed at the rate of 1 K/hour in all processes mentioned above. The contents were pressurized or depressurized without changing the total amount of substances by use of a volume controller. The optical high-pressure cell, approximately 0.2 cm^3 in volume, has a pair of sapphire windows, and the maximum working pressure is about 500 MPa.

The study of phase behavior reveals that the hydrate crystal compressed at supersaturated pressures never loses stability during the heating process until it reaches the equilibrium temperature of the maximum pressure, and that the hydrate crystal is reformed from the aqueous solution at F where the temperature

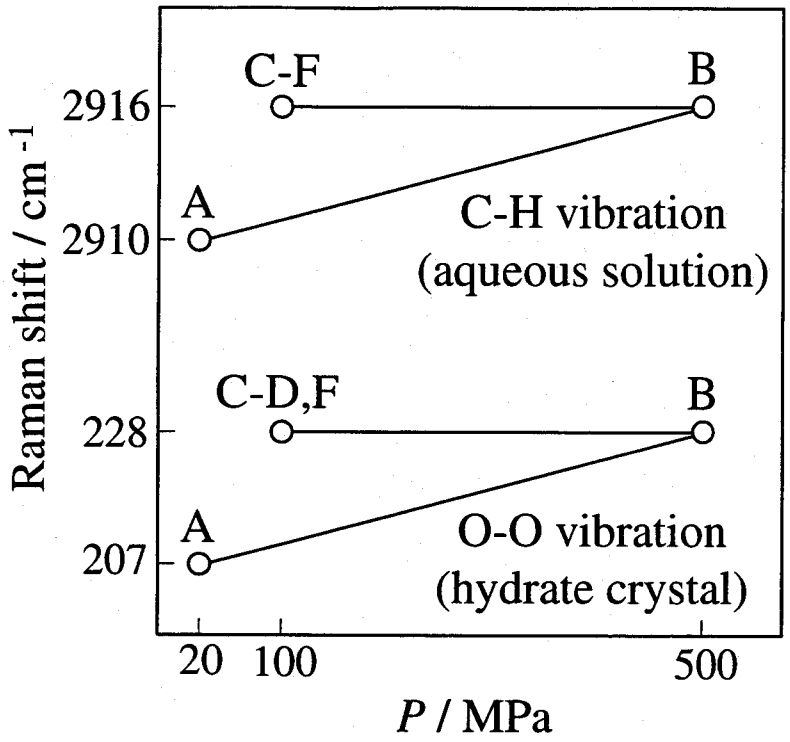

Fig. 5-2 Pressure effect on Raman shifts. Each symbol (A-F) corresponds to that of Fig. 5-1.

is 15 K higher than the equilibrium temperature for 100 MPa.

5.1.3 Raman spectroscopy

The single crystal of methane hydrate was analyzed by *in situ* Raman spectroscopy using a laser Raman microprobe spectrometer. The Raman shifts obtained in the whole process are given in **Fig. 5-2**. Both of the Raman shifts of the A-B process agree well with those of previous equilibrium data (Nakano *et al.*, 1999). It is one of the most interesting findings that all vibration energies are held constant at those of B (the maximum pressure) during the B-D process. In particular, the C-H stretching vibration energy in the aqueous solution is kept constant during the B-F process. It is also noticeable that the O-O and C-H vibration energies of the hydrate crystal which is reformed at F (15 K higher than the equilibrium temperature) are equivalent to those of B (the maximum pressure). Once the residual vibration energy in the aqueous solution is released at a higher

temperature than E, the hydrate crystal is never reformed until the equilibrium point C for 100 MPa.

Summary

The important findings in this study are summarized as follows: the hydrate crystal annealed at the maximum pressure remembers the compression in the hydrate S-cage until the higher equilibrium temperature for the maximum pressure is reached; this is the intrinsic nature of hysteresis in the hydrate dissociation; the hydrate S-cage-like structure in the aqueous solution also remembers the compression until the residual energy is released or the so-called activation energy is given by heating; therefore, the hydrate crystal compressed by the maximum pressure is always reformed at the equilibrium temperature for the maximum pressure; this is the intrinsic nature of hysteresis in the hydrate reformation. These findings suggest that the experimental procedure of isobaric temperature-swing instead of isothermal pressure-swing is effective for avoiding troublesome hysteresis in the stability boundary measurement. They also suggest the possibility that methane hydrate core recovered from deep-sea sediments will reveal information about the earth's natural history.

Literature Cited

Kvenvolden, K.A., "Methane Hydrate -A Major Reservoir of Carbon in the Shallows Geosphere?" *Chem. Geol.*, **71**, 41-51 (1988)

Nakano, S., M. Moritoki and K. Ohgaki, "High-Pressure Phase Equilibrium and Raman Microprobe Spectroscopic Studies on the CH_4 Hydrate System," *J. Chem. Eng. Data*, **44**, 254-257 (1999)

Nakano, S., M. Moritoki and K. Ohgaki, "High-Pressure Phase Equilibrium and Raman Microprobe Spectroscopic Studies on the CO_2 Hydrate System," *J. Chem. Eng. Data*, **43**, 807-810 (1998)

Ohgaki, K., T. Takano and M. Moritoki, "Exploitation of CH_4 Hydrates under the Nankai Trough in Combination with CO_2 Storage," *Kagaku Kogaku Ronbunshu*, **20**, 121-123 (1994)

Sloan, E.D. Jr.; Clathrate Hydrates of Natural Gases, p.94-95, Dekker, New York, U.S.A.(1990)

General Conclusion

In this thesis, the contents can be divided into three groups, which are the phase behavior, cage - occupancy and pressure - hysteresis for gas hydrates. All these results are the very fundamental information in order to carry out every practical application using gas hydrates, such as the methane exploitation from natural-gas hydrate, the heat storage and the desalination of sea water.

Phase behavior

In Chapter I, the three-phase coexisting curves for the trifluoromethane hydrate system were measured in a temperature range from 283 to 302 K and pressure range up to 72 MPa. The invariant quadruple point of $Q_2(H+L_1+L_2+G)$ is located at 292.25 K and 4.07 MPa. The (L_1+L_2+G) curve terminates at the invariant critical end point $(L_1+L_2=G)$ of 299.44 K and 4.85 MPa. The overall enthalpy change of hydration for the trifluoromethane shows weak temperature-dependency and becomes a continuous line in the $(H+L_1+G)$ and $(H+L_1+L_2)$ regions.

In Chapter II, the thermodynamical stability boundaries for the xenon hydrate system were measured in a temperature range from 290 to 320 K and pressure range up to 70 MPa. The invariant critical end point$(H+L_2=G)$ is located at 289.76 K and 5.86 MPa as the terminal point of $(H+L_2+G)$ curve. The three-phase coexisting curve of $(H+L_1+F)$ shows the characteristic "S-shape" curve in the *p-T* projection although the system has no quadruple point Q_2. It would be caused by the anomalous critical phenomena around the critical end point and slightly higher temperature region. The thermodynamic study on the pure xenon hydrate system is the most essential in order to investigate the structure-H hydrate crystal composed of xenon as help-gas.

In Chapter III, the stability boundaries for the ethylene hydrate system were measured in a temperature range from 279 to 328 K and pressure range up to 465 MPa. The invariant critical end point $(H+L_2=G)$ is located at 282.73 K and 5.03 MPa as the terminal point of $(H+L_2+G)$ curve. The three-phase coexisting

curve of ($H+L_1+F$) shows the characteristic "S-shape" curve in the *p-T* projection.

In Chapter IV, the stability boundaries for the cyclopropane hydrate system were measured in a temperature range from 278 to 320 K and pressure range up to 460 MPa. An intrinsic point of the quadruple point ($H + L_1 + L_2 + G$) at 289.46 K and 0.56 MPa has been observed. There is no structural transition (structure-I to structure-II) of cyclopropane hydrate in the whole range.

In the language of pressure-temperature projection, the phase diagrams of gas hydrate systems can be divided broadly into two groups, depending on the invariant quadruple points of $Q_1(H+S_1+L_1+G)$ and $Q_2(H+L_1+L_2+G)$. The type-q_1 diagram corresponds to only one quadruple point Q_1, while the type-q_2 diagram has two quadruple points of Q_1 and Q_2. When the critical temperature of the guest molecule is a primary index for determining the type of phase diagrams, ethylene (282.4 K), xenon (289.7 K), trifluoromethane (299.3 K) and CO_2 (304.1 K) would lie in the transitional zone between the type-q_1 and the type-q_2. The ethylene and xenon hydrate systems are identified to belong to the type-q_1 while the CO_2 and trifluoromethane hydrate systems belong to the type-q_2. The important finding is that trifluoromethane hydrate system is the border one having a quadruple point Q_2 in a series of critical temperatures of known guest species. It is also identified that xenon hydrate system is the opposite border one of no quadruple point.

Cage - occupancy

The laser Raman microprobe spectroscopic studies were applied in order to investigate the structures of gas hydrates. In Chapters III and IV, the Raman - active intramolecular vibrations of ethylene and cyclopropane were measured in the hydrate, saturated guest fluid and saturated water phases. Also, the O-O intermolecular vibration among the water molecules in the single crystal of each hydrate was measured.

It is found that the Raman spectrum of each intramolecular vibration mode for the ethylene molecule splits into double peaks in the hydrate phase, while a single peak is detected in both the saturated ethylene fluid and saturated water phases. The split of the Raman peak in the hydrate phase indicates that the

ethylene molecules are entrapped under the different energy conditions, that is, the ethylene molecules occupy both the S- and M-cages. This is the first evidence for the S-cage occupancy of the ethylene molecule.

The cage-occupancy for the cyclopropane hydrate system was discussed. In the pressure range lower than 200 MPa, a single Raman peak is detected for the symmetric ring-stretching vibration in the cyclopropane hydrate phase. As the pressure is raised, on the contrary, the Raman spectrum splits into double peaks, while a single peak was detected in both the saturated water and liquid cyclopropane phases under the whole pressure region. The Raman-peak intensity ratio ($I_{\text{S-cage}}$ / $I_{\text{M-cage}}$) of the cyclopropane molecules becomes linearly large as the compression and becomes zero around 200 MPa. These findings reveal that the cyclopropane molecule is able to be entrapped into S-cage in the pressure range above 200 MPa while the S-cage is perfectly vacant in the lower pressure region.

The intramolecular stretching vibration energy in the S-cage, aqueous solution and the M-cage decrease in that order for the ethylene hydrate system. The first two of them increase monotonically with pressure, however the energy in the M-cage is almost independent of pressure. For the cyclopropane hydrate system, the symmetric ring-stretching vibration energy shows similar behavior, except that the energy in the M-cage is larger than that of aqueous solution. They suggest that the hydrogen-bonded water cage shrinks gradually by pressurization and that the free volume around the guest molecule in the aqueous solution and the S-cage becomes smaller. On the other hand, it seems that the free volume in the M-cage is still large enough for the ethylene or cyclopropane molecule in spite of the cage shrinkage.

The O-O vibration energy in the ethylene hydrate shows stronger pressure - dependence than that in the ethane and cyclopropane hydrates (type-A), though it is not as strong as that in the methane and CO_2 hydrate systems (type-B) as shown in **Figure**. The van der Waals diameter increases in the order of ethane (0.53 nm), ethylene (0.55 nm) and cyclopropane (0.58 nm), however, such sequence is different from that of free space which is estimated from the pressure - dependency of each O-O vibration energy in hydrate lattice. This discrepancy may be due to oblate shape of ethylene molecule. Therefore, the hydrate - cage

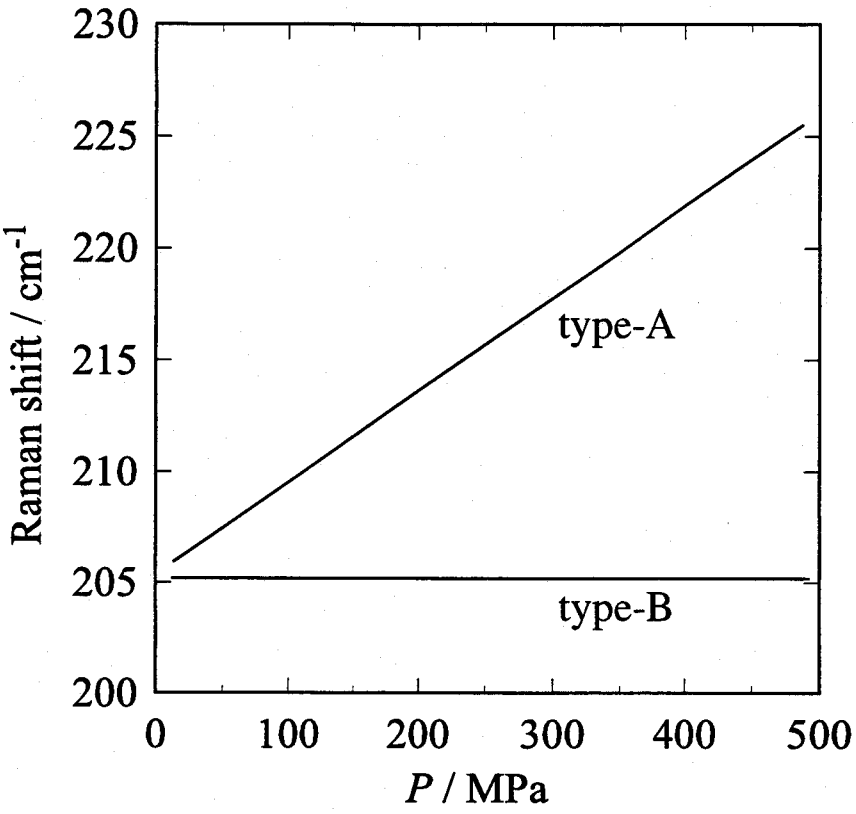

Figure Classification of the intermolecular O-O vibration energy. Type-A: dependence on pressure (methane and CO_2), Type-B: independence (ethane and cyclopropane). The ethylene, if anything, belongs to type-B.

occupancy and its pressure dependency must be discussed in consideration of the shape as well as the size of the guest molecule.

Pressure - hysteresis

In Chapter V, the pressure - hysteresis of the methane hydrate was first found by means of the Raman spectroscopy. The hydrate crystal annealed at the maximum pressure remembers the compression in the hydrate S-cage until the higher equilibrium temperature for the maximum pressure is reached. And the hydrate crystal is always reformed at that temperature. These are the intrinsic nature of hysteresis in the hydrate dissociation and reformation, respectively. On the condition where methane hydrates have dissociated, moreover, the dissolved

methane in the aqueous solution also remembers the compression until the residual energy is released by heating. This implies that the hydrate S-cage - like structure in the aqueous solution exists, which has been suggested by some investigators.

These findings suggest that the experimental procedure of isobaric temperature-swing instead of isothermal pressure-swing is effective for avoiding troublesome hysteresis in the stability boundary measurement. They also suggest the possibility that methane hydrate core recovered from deep-sea sediments will reveal information about the earth's natural history.

Suggestions for future work

Solid phase transition of gas hydrates

Three structures are well known in gas hydrates, structure-I, structure-II and structure-H. For a few years, it has been reported that the structure of gas hydrate crystal is changed by the pressure-temperature relation and the composition of mixed gases as well as the size and/or shape of guest molecules.

1. At higher pressure

Many investigators, Dyadin *et al.* (1997a, 1997b) and Hirai *et al.* (2000), have reported the structural changes of each methane, argon, xenon and krypton hydrate at high-pressure (0.6-1.5 GPa) via the Diamond Anvil Cell (DAC). These solid transition, however, is unclear and not examined well. Moreover, Londono *et al.* (1988) and Dyadin *et al.* (1999) amazingly report that helium and hydrogen, which have been too small to form hydrate crystals, can also form clathrate hydrates which have the ice-II-like structure. On the contrary, I suppose that such hydrogen and helium hydrates are not clathrate hydrates composed of hydrate cages.

We will construct new high-pressure optical cell, which has a maximum working pressure of 1 GPa and has a sample supply system. And then, we will confirm these solid phase transitions from the views of thermodynamics and Raman spectroscopic study. Such solid phase transition at high-pressure, needless to say, is essential on understanding the structure and nature of gas hydrates.

2. For the mixed gas hydrate system

Subramanian *et al.* (2000a and 2000b), Ballard and Sloan Jr. (2000) and Mooijer-van den Heuvel *et al.* (2000) report that the structure of the mixed gas hydrate crystals, which are made from both the relatively smaller (methane) and larger (ethane and trifluoromethane) molecules than the free void of S-cages, reverts from structure-I to structure-II and back to structure-I, while each single hydrate forms structure-I by themselves.

We are measuring the pressure - composition equilibrium relation in such

mixed gas hydrate system, methane + ethylene. When the spectroscopic studies will be applied in addition to the observation of such phase behavior, the hydration mechanism as well as the structural transition would be clear.

Preparation of structure-H hydrate crystal using " help gas"

In Chapter II, thermodynamical stability boundaries in the xenon hydrate system were measured. The relatively small molecules, methane and hydrogen sulfide as well as xenon, play an important role in forming structure-H hydrate crystal (Ripmeester *et al.*, 1987). The structure-H hydrates are composed of three-type cages. In the largest cage (U-cage), the large molecule, which can not form clathrate hydrate by itself, can be entrapped under the existence of small guest species. Therefore, such small guest species are called as "help-gases". Recently, the gas hydrate of structure-H has a significant impact on both natural-gas and petroleum industries, because structure-H hydrate is formed from components of a light naptha fraction as well as unleaded gasoline (Mehta and Sloan, 1996). Moreover, structure-H hydrate would be promising substances on the storage and transportation of the natural-gas (Khokhar *et al.*, 1998).

If we will investigate the structure-H hydrates with exploiting some techniques and experiences how we have ever investigated structure-I hydrates, we could epochally advance in knowledge of structure-H hydrates.

Literature Cited

Ballard, A. L. and E. D. Sloan Jr., " Structural Transitions in Methane + Ethane Gas Hydrates - Part II: Modeling beyond Incipient Conditions," *Chem. Eng. Sci.*, **55**, 5773-5782 (2000)

Dyadin, Y. A., E. G. Larionov, D. S. Mirinski, T. V. Mikina and L. I. Starostina, "Clathrate Formation in the Ar-H_2O System under Pressure up to 15000 bar," *Mendeleev Commun.*, 32-33 (1997a)

Dyadin, Y. A., E. Y. Aladko and E. G. Larionov, "Decomposition of Methane Hydrates up to 15 kbar," *Mendeleev Commun.*, 34-35 (1997b)

Dyadin, Y. A., E. G. Larionov, E. Y. Aladko, A. Y. Manakov, F. V. Zhurko, T. V. Mikina, V. Y. Komarov and E. V. Grachev, "Clathrate Formation in Water-Noble Gas (Hydrogen) Systems at High Pressures," *J. Struct. Chem.*, **40**(5), 790-795 (1999)

Hirai, H., T. Kondo, M. Hasegawa, T. Yagi, Y. Yamamoto, T. Komai, K. Nagashima, M. Sakashita, H. Fujihisa and K. Aoki, "Methane Hydrate Behavior under High Pressure," *J. Phys. Chem. B*, **104**, 1429-1433 (2000)

Khokhar, A. A., J. S. Gudmundsson and E. D. Sloan, "Gas Storage in Structure H Hydrates," *Fluid Phase Equilibria*, **150-151**, 383-392 (1998)

Londono, D., W. F. Kuhs and J. L. Finney, "Enclathration of Helium in Ice II: the First Helium Hydrate," *Nature*, **332**(10), 141-142 (1988)

Mehta, A. J. and E. D. Sloan, "Improved Thermodynamic Parameters for Prediction of Structure-H Hydrate Equilibria," *A. I. Ch. E. Journal*, **42**(7), 2036-2046 (1996)

Mooijer-van den Heuvel, M. M., C. J. Peters and J. de Swaan Arons, "Influence of Water - Insoluble Organic Components on the Gas Hydrate Equilibrium Conditions of Methane," *Fluid Phase Equilibria*, **172**, 73-91 (2000)

Subramanian, S., R. A. Kini, S. F. Dec and E. D. Sloan Jr., "Evidence of Structure II Hydrate Formation from Methane + Ethane Mixtures," *Chem. Eng. Sci.*, **55**, 1981-1999 (2000a)

Subramanian, S., A. L. Ballard, R. A. Kini, S. F. Dec and E. D. Sloan Jr., "Structural Transitions in Methane + Ethane Gas Hydrates - Part I: Upper Transition Point and Applications," *Chem. Eng. Sci.*, **55**, 5763-5771 (2000b)

List of Publications

1) Hysteresis in Dissociation and Reformation of Methane Hydrate Crystal
Kazunari Ohgaki, Takeshi Sugahara and Shinya Nakano
J. Chem. Eng. Japan, **32**(2), 235-236(1999)

2) Border Gas Hydrate System Having Quadruple Point of Hydrate + Two Liquids + Gas Phases
Takeshi Sugahara and Kazunari Ohgaki
J. Chem. Eng. Japan, **33**(1), 174-176(2000)

3) Phase Behavior of Xenon Hydrate System
Kazunari Ohgaki, Takeshi Sugahara, Masaru Suzuki and Hitoshi Jindai
Fluid Phase Equilibria, **175**(1-2), 1-6(2000)

4) Stability Boundary and Small Hydrate-Cage Occupancy of Ethylene Hydrate System
Takeshi Sugahara, Kentaro Morita and Kazunari Ohgaki
Chem. Eng. Sci., **55**(24), 6015-6020(2000)

5) Pressure Dependence of Small-Cage Occupancy in the Cyclopropane Hydrate System
Masaru Suzuki, Yuuki Tanaka, Takeshi Sugahara and Kazunari Ohgaki
Chem. Eng. Sci., in press

Others

1) NEMD Studies of Surface Heterogeneity Effects on Gas Permeation through Carbon Membranes
   Takeshi Sugahara, Shin-ichi Furukawa and Tomoshige Nitta
   Fifth Int. Conference on Inorganic Membranes, Nagoya, P-131(1998)

2) Non-Equilibrium MD Studies on Gas Permeation through Carbon Membranes with Belt-like Heterogeneous Surfaces
   Shin-ichi Furukawa, Takeshi Sugahara and Tomoshige Nitta
   J. Chem. Eng. Japan, **32**(2), 223-228(1999)

Acknowledgment

The author is greatly indebted to Professor Kazunari Ohgaki (Division of Chemical Engineering, Graduate School of Engineering Science, Osaka University) without whose guidance and helpful advise his study could not be a success.

The author is also grateful to the Professor Korekazu Ueyama (Division of Chemical Engineering, Graduate School of Engineering Science, Osaka University), Professor Tadashi Okada (Division of Chemistry, Graduate School of Engineering Science, Osaka University) for their helpful comments and suggestions to this work.

The author wishes to express sincere appreciation to Dr. Masato Moritoki for contriving experimental apparatus and to the other staff member of Ohgaki Laboratory, Lecturer Hiroshi Sato for offering advise on this study.

The author is also thankful to Mr. Masao Kawashima for his kind support in the GHAS (Gas Hydrate Analyzing System) room.

Thanks are given to the co-workers, Dr. Shinya Nakano, Mr. Kentaro Morita, Mr. Masaru Suzuki, Mr. Noriyuki Shimada, Mr. Yuuki Tanaka, Mr. Masanori Fukuda, Ms. Nur Awanis Hashim, Ms. Masumi Yamashita and all the other students of Ohgaki Laboratory for their collaboration.

Finally, the author would like to thank his parents, Akira Sugahara, Hifumi Sugahara, his sister Mayumi Sugahara, Dr. Takeshiro Shigeta, Mr. Masanori Kimura, Mr. Koreyoshi Munetomo, Mr. Kensaku Nakamura, Mr. Motoichi Murakami, Mrs. Noriko Murakami, Mr. Masaki Jo, Mr. Tatsushi Tokunaga and Mr. Ryo Umeki for their continuous and hearty encouragements.